ISTANBUL TECHNICAL UNIVERSITY ★ GRADUATE SCHOOL OF SCIENCE ENGINEERING AND TECHNOLOGY

Sod-ZMOF/MATRIMID MIXED MATRIX MEMBRANES FOR CO_2 SEPARATION

M.Sc. THESIS

Ayşe KILIÇ

Department of Chemical Engineering

Chemical Engineering Programme

JANUARY 2013

ISTANBUL TECHNICAL UNIVERSITY ★ GRADUATE SCHOOL OF SCIENCE ENGINEERING AND TECHNOLOGY

Sod-ZMOF/MATRIMID MIXED MATRIX MEMBRANES FOR CO_2 SEPARATION

M.Sc. THESIS

Ayşe KILIÇ
(506101007)

Department of Chemical Engineering

Chemical Engineering Programme

Thesis Advisor: Assoc. Prof. Dr. M. Göktuğ AHUNBAY

JANUARY 2013

İSTANBUL TEKNİK ÜNİVERSİTESİ ★ FEN BİLİMLERİ ENSTİTÜSÜ

CO$_2$ AYIRMA AMAÇLI *Sod*-ZMOF/MATRİMİD KARIŞIK MATRİSLİ MEMBRANLAR

YÜKSEK LİSANS TEZİ

Ayşe KILIÇ
(506101007)

Kimya Mühendisliği Anabilim Dalı

Kimya Mühendisliği Programı

Tez Danışmanı: Doç. Dr. M. Göktuğ AHUNBAY

OCAK 2013

Ayşe KILIÇ, a **M.Sc.** student of ITU **Graduate School of Science Engineering and Technology** student ID **506101007**, successfully defended the **thesis** entitled "*sod*-**ZMOF/MATRIMID MIXED MATRIX MEMBRANES FOR CO₂ SEPARATION**", which she prepared after fulfilling the requirements specified in the associated legislations, before the jury whose signatures are below.

Thesis Advisor :   **Assoc.Prof.Dr. M. Göktuğ AHUNBAY**   ....
İstanbul Technical University

Jury Members :   **Prof. Dr. Hüsnü ATAKÜL**   ....
İstanbul Technical University

Prof. Dr. Sacide ALSOY ALTINKAYA   ....
İzmir Institute of Technology

Date of Submission : 17 December 2012
Date of Defense :   16 January 2013

FOREWORD

Recently, membrane-based gas separation technology has attracted great interest; particularly studies on mixed matrix membrane development for enhancing the separation performance are gradually increasing. As a novel material, metal organic frameworks are seen as promising candidates for this purpose. In this thesis study, zeolite-like metal organic framework was synthesized and incorporated into a polyimide to develop mixed matrix membranes for CO_2 removal from natural gas.

TABLE OF CONTENTS

ABBREVIATIONS

CMS	**:** Carbon Molecular Sieve
DMF	**:** Dimethylformamide
DSC	**:** Differential Scanning Calorimetry
MMM	**:** Mixed Matrix Membrane
MOF	**:** Metal Organic Framework
SDA	**:** Structure Directing Agent
Sod	**:** Sodalite
Sod-**ZMOF**	**:** Zeolite-like Metal Organic Framework having a Sodalite topology
SEM	**:** Scanning Electron Microscopy
T_g	**:** Glass Transition Temperature
TGA	**:** Thermogravimetric Analysis
XRD	**:** X-Ray Diffraction
ZIF	**:** Zeolitic Imidazolate Framework
ZMOF	**:** Zeolite-like Metal Organic Framework

LIST OF TABLES

LIST OF FIGURES

Sod-ZMOF/MATRIMID MIXED MATRIX MEMBRANES FOR CO$_2$ SEPARATION

SUMMARY

Mixed matrix membranes (MMM) have attracted great interest for applications of gas separation as they combine the processability of polymeric membranes with superior permeability and selectivity of inorganic membranes. These hybrid membranes have been conventionally obtained by dispersing zeolites in a polymer matrix. In recent years, metal organic frameworks (MOF) have been introduced as a new class of microporous materials and they are seen as a good alternative to zeolites in mixed matrix membrane fabrication either for the ease of synthesizing and structural diversity. Furthermore, MOFs show good adhesion with polymers without requiring any surface treatment or coupling agent, since they have organic linkers having affinity with polymer chains.

In this work, *sod*-ZMOF (Zeolite-like Metal Organic Framework which has a *sodalite* topology) crystals were synthesized with the aim of developing polymer/MOF MMMs for CO$_2$/CH$_4$ separation. *Sod*-ZMOF was chosen as the dispersed phase due to its superior CO$_2$/CH$_4$ separation potential by means of having anionic framework and charge-compensating extra framework ions, which increase the interactions with guest molecules. In addition, Matrimid$^®$ was chosen as the continuous phase since it has high thermal stability, good permeability and selectivity properties as a commercially available polymer.

Sod-ZMOF crystals were synthesized by classical solvothermal method reported in the literature. The as-synthesized *sod*-ZMOFs were ion-exchanged with alkali Na$^+$ cations. The obtained X-Ray Diffraction (XRD) patterns were compatible with the ones published in the literature, which means the desired particles were synthesized successfully. Thermogravimetric analysis (TGA) of as-synthesized and ion-exchanged *sod*-ZMOF crystals indicated that the material was highly stable and the thermal stability of the material was conserved after alkali metal ion-exchange procedure.

Sod-ZMOF/Matrimid MMMs were prepared with the synthesized micron-size MOFs and annealed at 200 ºC for 48 hours. XRD patterns of the MMMs showed that *sod*-ZMOF crystals conserved their structural stability through the MMM preparation procedure. Scanning electron microscopy (SEM) images of MMMs showed a homogeneous dispersion of MOF particles in the polymer matrix and absence of interfacial voids at MOF/polymer interface. According to the pure gas permeability measurements, CH$_4$ and CO$_2$ permeabilities increased as the amount of incorporated MOF increased, while there was no significant change in the ideal selectivities. With 10 wt % MOF loading into the polymer matrix, single gas permeabilities increased approximately 35% compared with the pure polymer membrane.

CO$_2$ AYIRMA AMAÇLI *Sod*-ZMOF/MATRIMID KARIŞIK MATRİSLİ MEMBRANLAR

ÖZET

Karışık matrisli membranlar (KMM), polimerik membranların işlenebilirliği ile inorganik membranların üstün geçirgenlik ve seçicilik özelliklerini birleştirdikleri için gaz ayırma uygulamalarında büyük ilgi çekmektedirler. Bu hibrit membranlar yaygın olarak bir polimer matrisi içerisinde zeolitlerin dağıtılması ile elde edilmektedir. Son yıllarda, metal organik kafesler (MOF) yeni bir mikrogözenekli malzeme sınıfı olarak tanıtılmış ve hem sentezlenmelerindeki kolaylık hem de yapısal çeşitlendirilebilirlikleri nedeniyle karışık matrisli membran yapımında zeolitlere iyi bir alternatif olarak sunulmuştur. Ayrıca MOFlar polimer zincirleriyle birleşme eğilimi gösteren organik bağlayıcılara sahip olduklarından, herhangi bir yüzey işlemine veya uyumlaştırıcı ajana ihtiyaç duymadan polimerle tutunabilmektedir. Literatürde birçok MOF çeşidi ile hazırlanan KMMlere ait çalışmalarda MOFların kısmi organik yapısı sayesinde polimerle çok iyi birleşebildiği ve çeşitli gaz çiftlerinin ayırma performansını artırdığı rapor edilmiştir.

Bu çalışmada, CO$_2$/CH$_4$ ayırma amaçlı polimer/MOF KMM yapımında kullanılmak üzere *sod*-ZMOF (*sodalit* topolojisine sahip, zeolit benzeri metal organik kafes) kristalleri sentezlenmiştir. Anyonik kafese ve moleküllerle olan etkileşimi artıran yük dengeleyici kafes dışı iyonlara sahip olmaları nedeniyle üstün CO$_2$/CH$_4$ ayırma potansiyelinden dolayı *sod*-ZMOF dağılan faz olarak seçilmiştir. ZMOFlarla ilgili daha önce çeşitli gaz adsorpsiyon çalışmaları yapılmış olmasına rağmen membran yapımında kullanılmaları ve gaz ayırma özelliklerinin incelenmesi deneysel olarak ilk defa bu çalışmada gerçekleştirilmiştir. Yüksek ısıl dayanıklılığa sahip olması, ayrıca seçicilik ve geçirgenlik özellikleri iyi olan ticari bir ürün olması nedeniyle polimer matrisi olarak Matrimid$^{®}$ 5218 seçilmiştir.

Sod-ZMOF kristalleri, literatürde bildirilen klasik solvotermal yöntemle sentezlenmiştir. Sentezlenen malzeme X-ışını toz difraktometre (XRD) ile analiz edilmiş ve literatürdeki çalışmalarla oldukça uyumlu bir XRD deseni elde edilmiştir. *Sod*-ZMOF kristalleri taramalı elektron mikroskobu (SEM) ile incelendiğinde, çok yüzlü düzenli taneciklerin oluştuğu ve tanecik boyutunun literatürde de belirtildiği gibi 50-200 μm arasında olduğu görülmüştür. Ancak polimer matrisi içerisine katılarak KMM hazırlanabilmesi için tanecik boyutunun daha küçük olması gerektiğinden, boyut küçültme için sentez koşullarında (sıcaklık, pH, reaksiyon süresi, vb.) değişiklikler yapılarak farklı denemeler yapılmıştır. Sentezde kullanılan nitrik asit (HNO$_3$) miktarı yarı yarıya azaltılarak yapılan deneme başarıyla sonuçlanmış, bu yöntemle tanecik boyutu 2-30 μm arasında dağılım gösteren *sod*-ZMOF kristalleri elde edilmiştir.

Sentezlenen *Sod*-ZMOF'un yapısında bulunan yük dengeleyici imidazolyum katyonları, literatürde belirtilen iyon değişimi yöntemi kullanılarak Na^+ katyonları ile değiştirilmiştir. İyon değişimi yapılan parçacıkların SEM görüntülerinde morfolojilerinin değiştiği gözlemlenmiş; fakat elde edilen XRD deseni ile yapısında bir bozunmanın gerçekleşmediği, kristalinitenin kaybolmadığı görülmüştür. Sentez sonrası ve iyon değiştirilmiş *sod*-ZMOF kristallerine ait termogravimetrik analiz (TGA) sonuçları, malzemenin yüksek ısıl dayanıma sahip olduğunu ve alkali metal (Na^+) ile yapılan iyon değişimi prosedürü sonrasında malzemenin termal dayanımını koruduğunu göstermiştir. TGA termogramları, malzemenin yaklaşık 280 ºC'ye kadar termal olarak stabil olduğunu göstermiştir.

Sentezlenen 2-30 µm boyutundaki *Sod*-ZMOF kristallerinin yapısal ve termal analizleri tamamlandıktan sonra %5 ve %10 *sod*-ZMOF katkılı KMMler hazırlanmıştır. *Sod*-ZMOF parçacıkları manyetik karıştırma ve ultrasonik banyo kullanılarak dimetilformamid (DMF) içerisinde iyice dağıtıldıktan sonra Matrimid® ilave edilerek iyice çözünmesi sağlanmıştır. Elde edilen film çözeltisi, film aplikatörü yardımıyla cam/ayna yüzeye dökülerek döküm-evaporasyon yöntemi ile film elde edilmiştir. Oluşan film, analizlere ve gaz geçirgenlik ölçümlerine başlamadan önce 200 ºC'de 48 saat bekletilerek tavlanmıştır. Tavlama sonrasında elde edilen membranların kalınlıkları 45-65 µm arasında bulunmuştur. Daha sonra membranların saf gaz (CO_2 ve CH_4) geçirgenlikleri 35 ºC sıcaklıkta sabit hacim-değişken basınç yöntemi ile ölçülmüştür.

Sod-ZMOF kristallerinin membran hazırlama sürecinde (gerek film çözeltisi içinde mekanik karıştırma gerekse tavlama işlemi sırasında yüksek sıcaklıklarda) zarar görüp görmediğini anlamak için katkılı membranlara ait XRD desenleri elde edilmiş, analiz sonucunda *sod*-ZMOF taneciklerinin bu süreçte kristal yapısını kaybetmediği görülmüştür. KMMlerin SEM görüntüleri, MOF taneciklerinin polimer matrisi içerisinde homojen bir şekilde dağıldığını ve MOF/polimer arayüzünde boşlukların olmadığını göstermiştir. Bu sonuçlar, beklendiği gibi *sod*-ZMOF kristallerinin herhangi bir yüzey uyumlaştırıcı işleme gereksinim duymadan kendiliğinden polimere çok iyi yapıştığını ve kusursuz KMMler oluşturulabileceğini göstermiştir.

Tavlama işlemi sonrasında saf Matrimid ve karışık matrisli membranlarda hapsolan çözücü (DMF) kalıntısını tayin etmek için TGA analizleri yapılmıştır. DMF'in kaynama noktası olan 153 ºC'ye kadar membranlarda dikkate değer bir kütle kaybı görülmemiştir. Buna göre, tavlama işlemi ile çözücünün hemen hemen tümüyle uzaklaştırılabildiği görülmüştür. Diğer yandan, önemli bir kütle kaybı görülmese de *sod*-ZMOF katkılı membranlarda bu sıcaklığa kadar olan kaybın daha fazla olduğu görülmüştür. Bu durum da, membranların yapısına katılan *sod*-ZMOF taneciklerinin sahip oldukları geniş gözeneklerde bir miktar çözücünün hapsolmuş olabileceğini göstermiştir. Ayrıca *sod*-ZMOF'un organik yapısının yaklaşık 380 ºC'de tamamen kaybolmasına bağlı olarak katkılı membranlarda 300-400 ºC arasındaki kütle kaybının saf membranlara göre daha fazla olduğu görülmüştür. Diferansiyel taramalı kalorimetri (DSC) analizleri ile KMMlerin camsı geçiş sıcaklıkları (T_g) ölçülmüş ve saf matrimid membran ile kıyaslanmıştır. KMMlerin T_g değerleri saf matrimid membranın T_g değerine çok yakın çıkmıştır, aradaki birkaç derecelik farklar deneysel hata sınırları içerisinde yer aldığından ayrıca yorumlanmamıştır.

Saf gaz geçirgenlik ölçümlerinde, polimer matrisi içerisine katılan MOF miktarı arttıkça CH_4 ve CO_2 geçirgenlikleri artarken seçiciliklerde önemli bir değişim olmadığı görülmüştür. Saf matrimide kıyasla CO_2 geçirgenlikleri %5 *sod*-ZMOF katkısı ile %22 artarken, %10 *sod*-ZMOF katkısı ile %35 artış göstermiştir. *Sod*-ZMOF kristalleri 9.6 Å boyutunda oldukça geniş gözenek açıklığına sahip olduklarından, polimer matrisi içinde her iki gaz molekülünün de rahatlıkla geçebileceği yollar oluşturduğu ve bu nedenle geçirgenlikleri artırdığı düşünülmektedir.

Bununla birlikte, KMMlerin ideal CO_2/CH_4 seçicilikleri saf polimer membranla kıyaslandığında önemli bir değişiklik olmadığı, az miktarda düştüğü görülmüştür. Bu durum Maxwell modeli ile de açıklanabilir. Bu modele göre, polimer matrisi içerisine katılan malzemenin, membrandan geçirilen gazlara karşı polimerden daha geçirgen olması durumunda seçicilikte artış sağlanamayacağı öngörülmektedir. Buna karşılık seçicilikteki düşüşün ihmal edilebilecek kadar küçük olması, SEM görüntülerinden yola çıkılarak yapılan yorumları doğrular nitelikte olup membran yapısında polimer/MOF arayüzünde seçici olmayan boşlukların bulunmadığını açıklamaktadır.

Diğer taraftan, Na^+ ile iyon değişimi yapılan *sod*-ZMOF'la hazırlanan KMMde, yukarıda söylenenlerin aksine seçiciliğin az da olsa arttığı görülmüştür. Bu farklılığın, yapıya katılan Na^+ iyonlarının CO_2 molekülleriyle elektrostatik etkileşimi artırması ile meydana geldiği düşünülmüştür. Daha önce literatürde yapılan adsorpsiyon çalışmalarında da, Na^+ iyonlarının güçlü kuadrupol momente sahip olan CO_2 moleküllerine karşı ilgisinin yüksek olduğu ve bu nedenle Na^+ ile iyon değişimi yapılan *sod*-ZMOF'ların adsorpsiyon kapasitesinde artış gözlendiği söylenmiştir.

Sonuç olarak, *sod*-ZMOF tipi MOFlar poliimid CO_2 ayırma membranlarının performanslarını artırmada umut vaat etmektedirler. İleriki çalışmalarda yüksek oranda *sod*-ZMOF katkısı içeren karışık matrisli membranların gaz karışımlarını ayırmadaki performanslarının incelenmesi, bu malzemelerin kullanım potansiyelini ortaya koyacaktır.

1. INTRODUCTION

Traditional gas separation processes are cryogenic distillation, absorption and pressure swing adsorption. From the economic perspective, these processes are typically high energy consuming and most of them are complex processes that require large-scale equipments, which increase the capital and operating cost. The membrane systems are more energy-efficient compared with conventional separation methods [1-4]. They offer many advantages such as ease of operation, high stability and high efficiency, low capital and operating costs, low energy requirement, flexible size and being environmentally friendly. By means of these features, industrial gas separation using membranes have been of great interest over the past few decades. Oxygen enrichment or inert gas (nitrogen) generation from air, hydrogen recovery from syngas, separation and recovery of CO_2 from biogas and natural gas, greenhouse gas capture from air and the removal of volatile organic compounds from waste streams are some current applications of gas separation membranes [5-10].

In this section, a general overview of the membrane-based gas separation theory is obtained. Then, importance of natural gas separation is emphasized and current situation of separation processes are exhibited. At the end, purpose of the thesis is clarified.

1.1 Membrane-Based Gas Separation

The membrane is a thin barrier that separates two phases by restricting transport of some components in a selective manner. A driving force, which can be concentration, pressure, temperature or electrical potential difference, provides differential transport through a membrane [5, 7]. A schematic representation of a gas separation membrane is shown in Figure 1.1. Currently, a large number of materials can be used for membrane fabrication, including polymers, zeolites, silica and carbon molecular sieves. Membrane module types can be classified as flat sheets (plate-in-frame or spiral wound configurations), tubes, and hollow fibers [11].
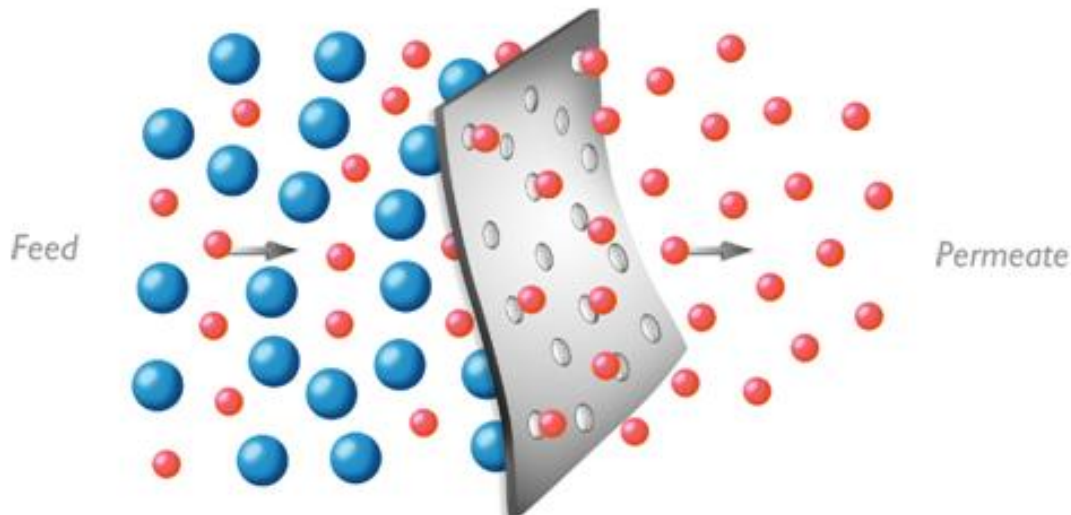
Figure 1.1 : Schematic presentation of a gas separation membrane [12].

Although membrane-based gas separation has been widely used for industrial applications only since 1980s, the history of this technology may be attributed back over nearly two centuries [3, 13]. In 1829, Thomas Graham, a Scottish chemist, carried out the first recorded experiments when he observed gaseous osmosis for the air-carbon dioxide system through a wet pig bladder [3, 14]. In 1866, he proposed "solution-diffusion" theory for gas permeation through a membrane, which is still the accepted model for gas transport in polymeric membranes [3, 4, 13]. Afterwards, in 1879, Von Wroblewski evaluated Graham's model and developed a formula for the permeability coefficient as the penetrant flux multiplied by the membrane thickness divided by the trans-membrane pressure. He also defined the permeability of a gas as the product of diffusion and solubility coefficients, which is now a crucial model in membrane permeation. Kayser indicated the validity of Henry's law in 1891 for the absorption of carbon dioxide in natural rubber. Many other fundamental scientific studies and contributions related with the development of membrane-based gas separation were also performed by several scientists (Knudsen, Shakespear, Daynes and Barrer among many others) in the twentieth century [3, 4].

The first practical application of membrane-based gas separation was in the years between 1943 and 1945, as a part of the Manhattan Project. In this project, finely microporous metal membranes were used to separate $U^{235}F_6$ from $U^{238}F_6$ in a separation facility built in Tennessee, USA. This plant represented the first large-scale use of gas separation membranes and for the next 40 years, it remained as the largest membrane separation plant of the world. Unfortunately, the project was

unique and very secret so this application had basically no influence on the long-term development of membrane-based gas separation [13]. The golden age of membrane science started in 1960 with the invention of the asymmetric phase-inverted membranes made of cellulose acetate by Loeb and Sourirajan. Then in 1980, Permea produced the first commercially feasible gas separation membrane, which was a hydrogen separation membrane launched as Prism®. This successful application presented an attractive alternative for separation applications of different gas mixtures and accelerated the development of novel membrane materials [3, 4, 13-16]. The significant milestones in the chronological development of membrane-based gas separation technology are shown in Figure 1.2.
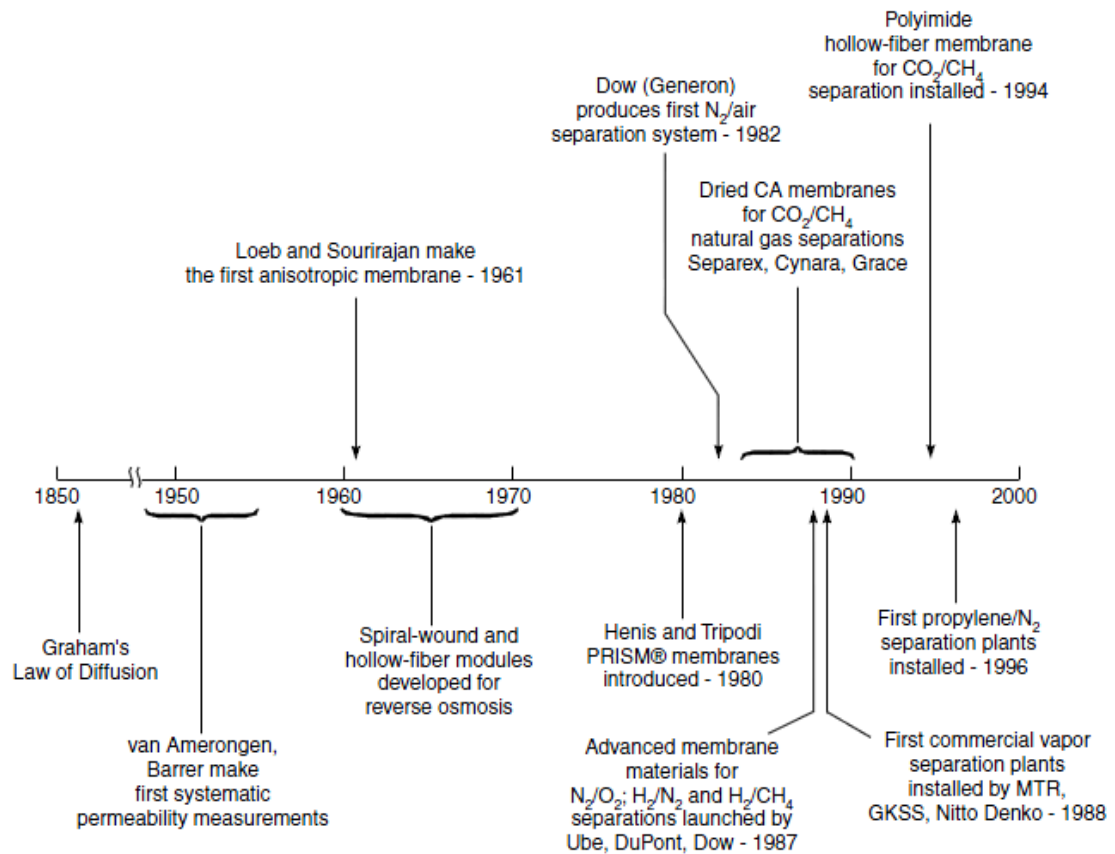
Figure 1.2 : Historical development of membrane-based gas separation [13].

Today, membrane-based gas separation systems have been applied in a large number of industrial sectors. Membrane technology competes well with other conventional separation methods due to some specific characteristics and inherent advantages such as [4, 17]:

➢ Ease of installation and operation,

- ➢ Low capital investment and low energy consumption,

- ➢ Space and weight efficiency (being compact and modular),

- ➢ Simplicity and economic viability of scale-up or scale-down (being flexible),

- ➢ Operation under mild conditions,

- ➢ Possibility of being combined with other separation systems for influential hybrid processes,

- ➢ Being environmentally friendly.

1.2 Natural Gas Purification

Natural gas is one of the most significant energy sources of the world. When compared with other conventional fossil fuels such as coal and crude oil, it is evaluated as an environmentally friendly fuel due to lower emission rates of carbon dioxide, nitrous oxide, etc. [18, 20]. The emission levels of natural gas and other fossil fuels can be seen in Table 1.1. With respect to these favorable features, its usage is becoming widespread and the demand for natural gas has been increasing every year [11, 20].

Table 1.1 : Emission levels for natural gas and other fossil fuels [22].

Pollutant	Natural Gas	Oil	Coal
Carbon dioxide	117000	164000	208000
Carbon monoxide	40	33	208
Nitrogen oxides	92	448	457
Sulfur dioxide	1	1122	2591
Particulates	7	84	2744
Mercury	0.000	0.007	0.016

Natural gas is a mixture of hydrocarbon gases (mainly CH_4) including some impurities such as nitrogen (N_2), carbon dioxide (CO_2) and hydrogen sulfide (H_2S). As natural gas is extracted from wells at different compositions and pressures, the raw natural gas composition varies from source to source. The CH_4 content is generally in the range of 75-90% [10, 19-21]. Table 1.2 shows a generalized composition for natural gas obtained from different types of reservoirs.

Prior to transportation in the pipeline and domestic use of natural gas, it requires some treatment mainly such as removal of CO_2, N_2, H_2S and H_2O [10, 14, 20]. Carbon dioxide content of the natural gas is usually at high levels, varying in a wide range from 4 to 50%. Even in some natural gas fields as much as 70% CO_2 exists [10, 23]. Carbon dioxide causes a reduction in heating value of the gas and also it becomes acidic and corrosive in the presence of water, leading to problems in transportation pipeline [14, 25]. Correspondingly, before the delivery to a pipeline, CO_2 content has to be reduced to below 2% to meet sales specifications [24]. The most commonly used conventional method for CO_2 separation from natural gas (sweetening) is amine absorption process [11, 25, 26]. In this process, briefly CO_2 is absorbed into the aqueous solutions of alkanolamines. Monoethanolamine (MEA), diethanolamine (DEA) and methyldiethanolamine (MDEA) are the most widely used amines in the process. Although amine absorption is a mature method for CO_2 capture, it has some drawbacks such as being high energy consuming, requiring very large areas for process equipments and problems arising from operating and disposal of corrosive amine solutions [11, 27, 28].

Table 1.2 : Typical composition of natural gas before purification, and sales specifications, [10, 16].

Gas	Chemical Formula	Amount	Sales specifications
Methane	CH_4	70-90	90%
Ethane	C_2H_6		< 3 - 4%
Propane	C_3H_8	0-20[a]	
Butane	C_4H_{10}		~3%[b]
Carbon dioxide	CO_2	4-50	< 2%
Oxygen	O_2	0-0.2	-
Nitrogen	N_2	0-5	< 4%
Hydrogen sulphide	H_2S	0-5	< 4 ppm
Water	H_2O	Saturated	< 100 ppm
Rare gases	Ar, He, Ne, Xe	Trace	-

[a] Total amount of C_2-C_4
[b] Total amount of C_3-C_5

Recently, membrane-based gas separation processes have started to be preferred as they are simple, energy-efficient and environmentally friendly operations [11]. There are examples for the application of membrane-based gas separations in commercial-scale. Especially polymeric membranes such as cellulose acetate, polyimides and polyamides are used for separation CO_2 from CH_4 [25, 29, 30]. From the energy and

environmental perspective, membrane technology is expected to become widespread over the following years [31]. In parallel with, development of new materials and procedures will be required to meet the desired specifications.

1.3 Research Objectives

The fundamental aim of this thesis is to develop efficient and commercially viable mixed matrix membranes for separation of CO_2/CH_4 gas mixtures (natural gas purification). To achieve this purpose, the below steps are followed:

➢ Selecting the proper polymer and MOF for the desired purpose,

➢ Synthesizing *sod*-ZMOF crystals having a sodalite topology for using in mixed matrix membrane preparation,

➢ Characterizing the structural and thermal properties of synthesized *sod*-ZMOF particles,

➢ Constituting and developing an appropriate membrane preparation method to obtain defect-free composite membranes,

➢ Characterizing the morphology, thermal properties and gas separation features of pure and mixed matrix membranes,

➢ Comparing the performances of pure and mixed matrix membranes,

➢ Investigating the effect of ion exchange procedure to sod-ZMOF characteristics and to gas separation performance of membranes containing ZMOF.

The thesis is organized according to these objectives. Chapter 2 gives some background about the gas transport mechanisms of membranes and also membrane materials. Chapter 3 explains the materials used and experimental methodology. Chapter 4 clarifies the results and discussions. Finally, Chapter 5 concludes the discussions and presents the feasible future studies.

2. THEORY AND BACKGROUND

In the concept of gas separation, membranes act as semi-permeable barriers which separate one or more gases from a gas mixture to generate a permeate stream rich in a specific gas. The simplicity and energy efficiency of membrane processes make them highly attractive compared to complex and energy-intense conventional gas separation methods such as cryogenic distillation and absorption [32-34].

This chapter provides a theoretical background into gas transport mechanisms and performance characterization in membranes, covers the literature review on the materials used in membrane fabrication, briefly introduces mixed matrix membranes and then draws attention to metal organic frameworks, which are novel materials started to be used in mixed matrix membrane preparation.

2.1 Gas Transport Through Membranes

The most significant feature of gas separation membranes is their ability to control the permeation rate of different species. The first mechanism for this selective transport was "solution-diffusion model", which was developed by Thomas Graham [13, 14]. There are five possible mechanisms for gas transport through membranes: Knudsen diffusion, molecular sieving, solution-diffusion, surface diffusion and capillary condensation.

Knudsen diffusion takes place in porous membranes when gas molecules are passing through pores of the membrane that are small enough to prevent bulk diffusion. In this mechanism, separation occurs due to the difference in the mean free path of gas molecules, resulting from collisions with pore walls [14, 32].

Molecular sieving takes place when gas mixtures are separated by size exclusion. According to this model, the diffusion of smaller gas molecules occurs faster while larger gas molecules are restrained through membranes with carefully controlled pore size relative to the kinetic diameters of the permeating gas molecules [32]. Therefore, separation of a gas pair with molecular sieving can be succeeded when

membrane has pore diameters between the kinetic diameters of two penetrant gas molecules.

Solution-diffusion mechanism takes place in polymeric membranes, which are typically non-porous. According to this model, gas transport is considered to consist of three basic steps: Firstly gas molecules from the upstream gas phase sorb into the membrane, then they diffuses through the membrane cross-section and finally they desorb into the downstream side. This mechanism is explained comprehensively in section 2.2 [3, 14, 32].

Surface diffusion takes place in porous membranes by the migration of adsorbed gas molecules through the pore walls. The level of interaction between the pore surface and adsorbed gas molecules determines the surface diffusion rate and separation efficiency.

Capillary condensation also takes place in porous membranes when the adsorbed gas molecules undergo partial condensation within the pores due to the vapour pressure drop. Diffusion of this condensed component through the pore becomes faster than gases and the condensable gas can be separated by this way [32].

Among these methods, Knudsen diffusion, molecular sieving and solution-diffusion are usually more effective. These separation mechanisms are illustrated in Figure 2.1.
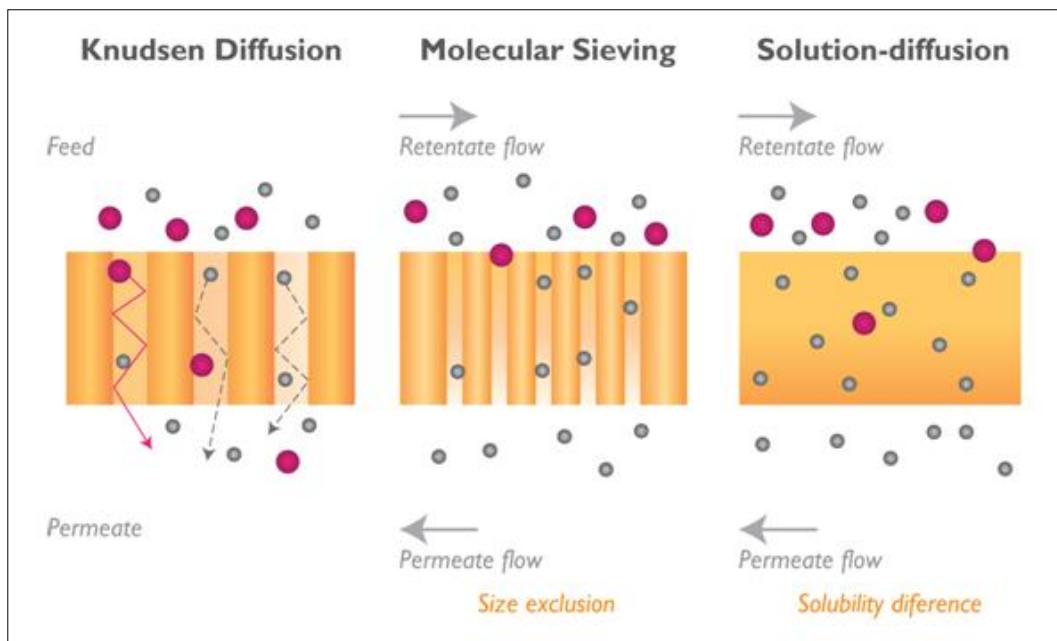
Figure 2.1 : Schematic representation of three most common possible mechanisms for membrane-based gas separation [35].

2.2 Polymeric Membranes for Gas Separation

The most dominantly-used mechanism for gas permeation through dense polymeric membranes is "solution-diffusion" model [36-38]. According to this model, the permeation of of gas molecules is controlled by two main mechanisms: solubility and diffusivity. Solubility can be defined as the number of gas molecules dissolved in the membrane while diffusivity is the mobility of gas molecules through the molecular-scale gaps in membrane cross-section [4,39]. Permeability (P) is a measure of the membrane's ability to permeate gases and it is basically described as the product of solubility coefficient (S) and diffusion coefficient (D), which is described in Equation **2.1.**

$$P = S \times D \tag{2.1}$$

In SI system, the unit of P is mol·(m^2·s·Pa), but the most commonly used unit for P is Barrer, which stands for 10^{-10} cm^3(STP)·cm/cm^2·s·cmHg. The permeability coefficients of different gases in polymer membranes generally vary in a wide range between 10^{-4} and 10^4 Barrer [36, 40, 41].

Gas transport through a dense polymer membrane is described by Equation **2.2**

$$j_i = \frac{D_i S_i \left(p_{i_0} - p_{i_l} \right)}{l} \tag{2.2}$$

where j_i is the molar flux of component i (cm^3-STP/cm^2·s), l is the membrane thickness, p_{i_0} is the partial pressure of component i on the feed side and p_{i_l} is the partial pressure of component i on the permeate side [28]. This equation is also expressed as in terms of permeability coefficient, as it can be seen in Equation **2.3**

$$j = P \frac{\Delta p}{l} \tag{2.3}$$

where Δp is the pressure difference throughout the membrane. In other words, permeability is the gas flux across the membrane under the pressure difference (driving force) and normalized to the unit thickness of the membrane. Equation **2.4** represents this mathematically [36, 40].

$$P_i = \frac{j_i \, l}{\Delta p_i} \tag{2.4}$$

The separation performance of a membrane is measured by (perm)selectivity. It is the second key parameter for gas while permeability is the first one. The ideal selectivity of a polymer membrane for gas A over gas B named as $\alpha_{A/B}$, is mathematically the proportion of the permeability of gas A (P_A) to the permeability of gas B (P_B). It can be also written as the product of sorption selectivity (S_A/S_B) and diffusion selectivity (D_A/D_B) of the gas pair, as shown in Equation **2.5** [39, 40, 42]. Sorption selectivity shows the relative concentration of the components A and B within the membrane material and it is proportional to the relative condensability of components in the membrane. On the other hand, diffusion selectivity, which is also called as mobility selectivity, shows the relative motion of individual gas molecules of the components A and B, and it is proportional with the size of the permeant gas molecules [28].

$$\alpha_{A/B} = \frac{P_A}{P_B} = \frac{S_A}{S_B}\frac{D_A}{D_B} \qquad (2.5)$$

The above equation is especially useful for determining the ideal gas performance of membranes in single gas conditions, for permanent gases at relatively low pressure. For mixed gas streams including highly soluble gas streams such as CO_2 and hydrocarbons, it is more accurate to calculate the "actual" selectivity with the following equation **2.6**

$$\alpha^*_{A/B} = \frac{y_A/y_B}{x_A/x_B} \qquad (2.6)$$

where y_A and y_B are the mole fractions of the components A and B in the permeated stream while x_A and x_B are the corresponding mole fractions in the feed stream [11, 40].

Rate of diffusion and sorption through membranes depends on the state of the polymer material, whether the membrane is below or above its glass transition temperature (T_g) [14, 36, 39]. Below T_g, polymer is in glassy state and above T_g, it is in rubbery state. In other words, polymer material changes from glassy state to rubbery state when the temperature reaches T_g. When considered from this point of view, polymers can be classified as two main categories: rubbery and glassy, depending on the T_g. While rubbery polymers are soft and elastic as a result of movements in polymer chains, glassy polymers are rigid and hard because of prohibited movement of polymer segments [13]. Above the glass transition

temperature, the membrane material is also assumed to reach thermodynamic equilibrium [3, 39]. Diffusivity (mobility) is higher in rubbery state due to the thermal motion of the polymer segments. The thermal motion of the polymer molecules leads to the growth of temporary molecular-scale spaces (free volume) between the polymer chains and the permeant gas molecules jump through these tiny gaps. While the diffusivity coefficients of rubbery polymers are usually very high for many gases, their diffusivity selectivities are quite small. Consequently, these polymer materials should be preferred when solubility selectivity is dominant [3, 11, 13]. In glassy state, the mobility of polymer segments are very limited so this state is also called as frozen state. In this frozen state, inefficient chain packing and excess free volume exist in the polymer matrix due to being in non-equilibrium [3, 39]. Figure 2.2 indicates the polymer free volume and state as a function of temperature.
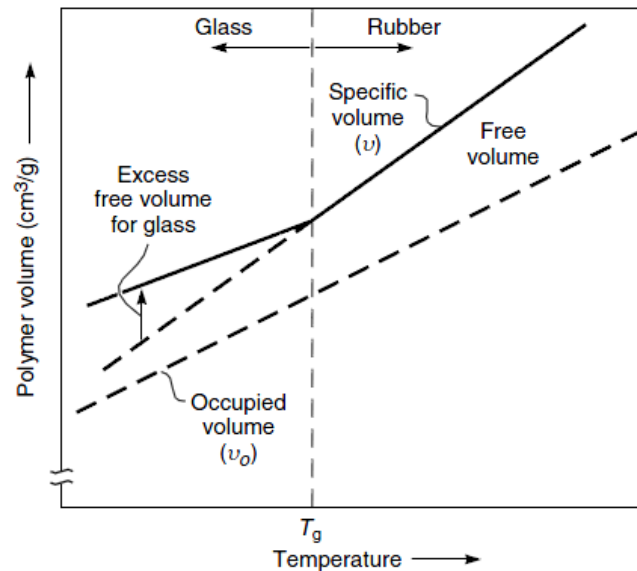
Figure 2.2 : The relation between specific volume and temperature for a typical polymer [13].

Solubility of gases in rubbery polymers is similar to the dissolution of gases in liquids. They are assumed to be in thermodynamic equilibrium and solubility of the gas in the polymer matrix generally obeys Henry's Law, which is shown below

$$C_D = k_D p \tag{2.7}$$

where C_D is the concentration of gas in the polymer matrix, k_D is the Henry's solubility constant for the particular polymer-gas pair (cm^3-STP/cm^3 polymer cmHg) and p is the partial pressure of the permeant gas. According to this equation, the gas

11

concentration in the polymer is linearly proportional to the external partial pressure [4, 14, 39].

On the other hand, the solubility of gases in glassy polymers obeys a more complex sorption isotherm, which named as dual mode sorption model [13, 14]. This model is a combination of Henry's Law and Langmuir sorption. This theory is shown in Equation **2.8** and the sorption isotherms are illustrated in Figure 2.3.

$$C = C_D + C_H = k_D p + \frac{C_H' bp}{1+bp}$$

(2.8)

where C is the total gas concentration in the polymer matrix, C_D is the gas concentration in the Henry type sites, C_H is the gas concentration in the Langmuir sites, C_H' is the Langmuir sorption capacity (the sorption capacity of the unrelaxed volume) and b is the Langmuir affinity constant (the ratio of rate constants of adsorption and desorption in the holes or defects). Indeed, C_D stands for the sorption of the diffusible species and C_H stands for the sorption in microvoids or defects [13, 14, 39].
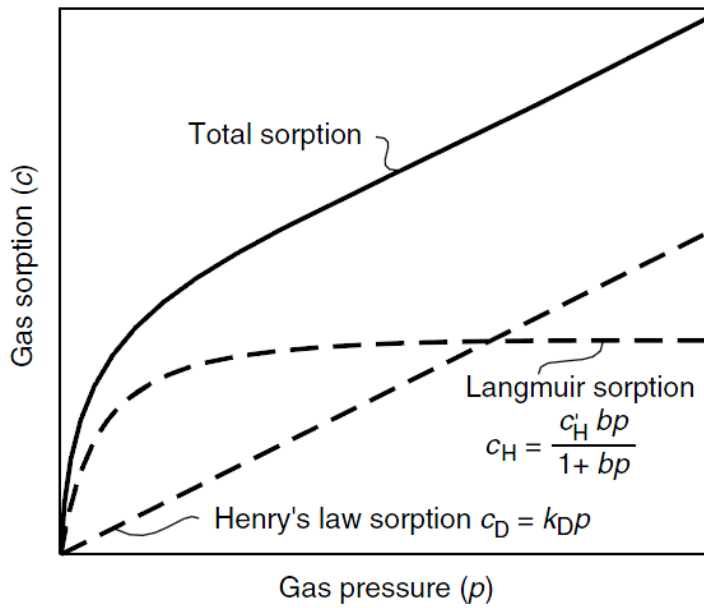
Figure 2.3 : Schematic represantation of Henry type, Langmuir type and dual mode sorption [13].

As the above figure indicates, Langmuir sorption dominates at lower pressures as the penetrant molecules prefer to fill the free volume. As pressure increases, the Langmuir sites (microvoids) reach the saturation limit and Henry's law sorption starts to play a larger role [11, 14].

For an efficient separation, polymers are desired to both have high permeability and high selectivity. Higher permeability decreases the required membrane area and thereby decreases the capital cost for the process while higher selectivity results in higher purity product gas. However, the performance of polymeric membranes is restricted by the trade-off upper bound that was initially published by Robeson in 1991. This trade-off relation was represented on the basis of a comprehensive literature research, quantifying all the permeation and selectivity data of different gas pairs for available polymer materials. According to this trade-off trend, there is an inverse relation between permeability and selectivity. Polymers with high selectivities commonly have low permeabilities and polymers with high permeabilities commonly have low selectivities [8, 42, 43]. Figure 2.4 presents the upper-bound for various gas pairs, with selectivity on the ordinate, and permeability of the more permeable gas, on the abscissa (in logaritmic scale).
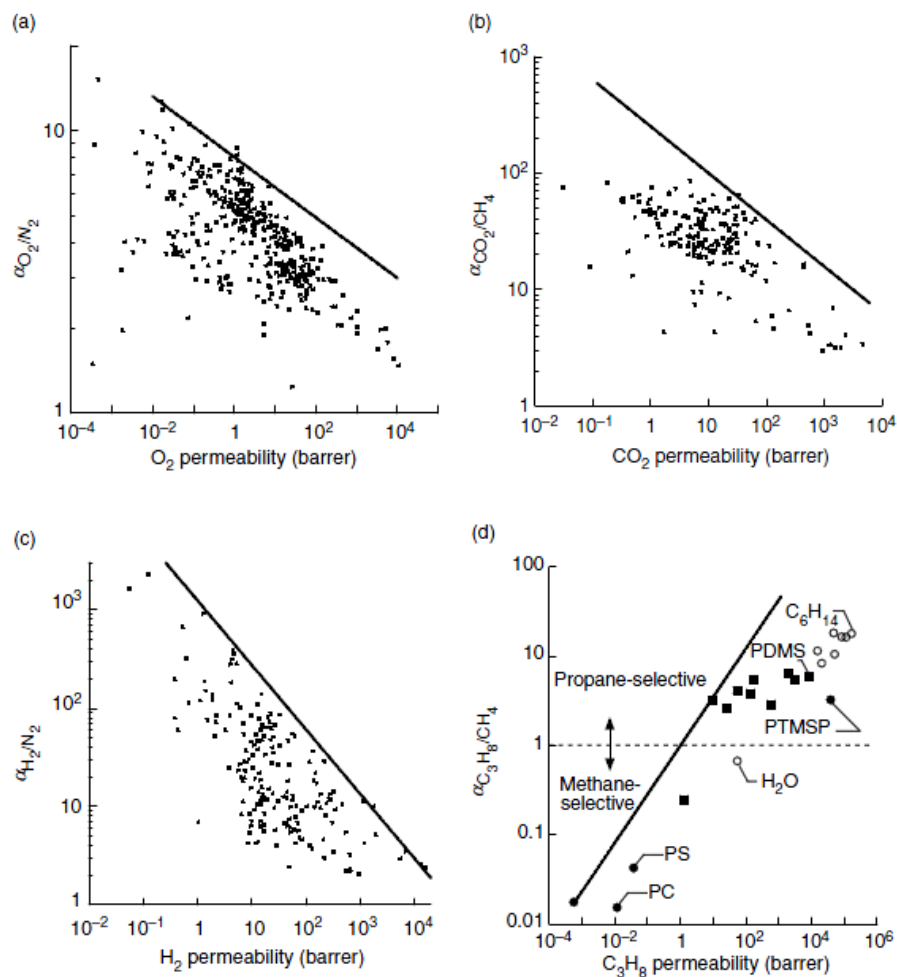
Figure 2.4 : Permeability/selectivity trade-off maps for: (a) O_2/N_2; (b) CO_2/CH_4; (c) H_2/N_2; (d) C_3H_8/CH_4 [36].

Robeson then reviewed these upper bounds with the presently available data in the literature and the upper bound positions shifted in 2008 [44]. Prior and present upper bound relationships for CO_2/CH_4 gas pair are shown in Figure 2.5. As seen on the figure, almost all of the available polymer materials (shown with dots) are under the trade-off line.
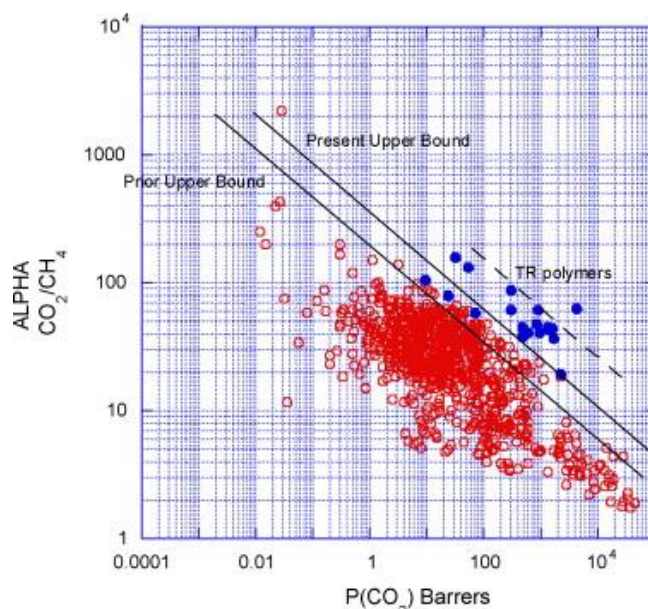
Figure 2.5 : Permeability/selectivity trade-off relationship for CO_2/CH_4 [44].

Membrane technology for CO_2 removal from natural gas started to be commercially used in 1980s and still it has been widely used for this purpose. Especially polymeric membranes have been preferred in industrial processes due to their processability and ease of fabrication. The most common polymer materials used for CO_2 removal are cellulose acetate, polyimides and perfluoropolymers [45]. Table 2.1 summarizes literature data for CH_4/CO_2 separation performance of several polymer membranes.

Table 2.1 : Single gas permeability and CO_2/CH_4 selectivity for several polymer membranes at 35ºC.

Polymer	Pressure (bar)	Permeability (Barrer)		CO_2/CH_4 Selectivity	Ref.
		CH_4	CO_2		
Cellulose acetate (CA)	0.27	0.21	5.96	29.07	[46]
6FDA-DAM:DABA	10	4.59	133	29	[23]
Matrimid 5218	2	0.15	5.39	35.93	[47]
Poly-[perfluoro(2-methylene-4-methyl-1,3-ioxolane)]	7.8	2	67	33.5	[48]

2.3 Inorganic Membranes for Gas Separation

The first large-scale inorganic membranes were developed in 1940s for separation of uranium isotopes to enrich uranium in Manhattan Project. The project was very secret as they were being developed for military purposes. Therefore, the usage of inorganic membranes started to be identified and become widespread with non-nuclear applications of them. In the 1970s, Union Carbide introduced Ucarsep[R] membranes, consisting of a thin layer of zirconia generated on the inner side of a tubular carbon. Then in the 1980s, both research-development and industrial application of inorganic membranes increased. Primarily with the Robeson trade-off trend being published, inorganic membranes started to become attractive due to their enhanced gas permeation and separation properties [37, 43, 49].

Inorganic membranes can be classified into two main categories: porous inorganic membranes and dense (non-porous) inorganic membranes. Ceramic membranes (e.g. alumina, silica, titania, glass), porous metals (e.g. stainless steel, silver), zeolite and carbon membranes are several examples of commercially used porous inorganic membranes. These membranes generally have high permeabilities but low selectivities. On the other hand, dense membranes such as palladium and its alloys have better selectivities but low permeabilities. Therefore, commonly porous inorganic membranes have been used for industrial applications. Studies have particularly focused on molecular sieve membranes such as zeolite, silica and carbon membranes, as they mostly lie above the Robeson trade-off line [37, 49]. Table 2.2 shows a brief literature overview of inorganic molecular sieve membranes for CH_4/CO_2 separation.

Table 2.2 : Single gas permeability and CO_2/CH_4 selectivity for several molecular sieve membranes.

Membrane	Temp. (K)	Permeance (10^{-8}/mol.m^2.s.Pa)		CO_2/CH_4 Selectivity	Reference
		CH_4	CO_2		
SAPO-34	295	0.46	66.0	143	[50]
DDR-type zeolite	298	0.11	30.0	280	[51]
Si(400)	298	0.07	22.8	326	[52]

As also seen from the table, zeolite and silica membranes possess high separation selectivities. A majority of them are in or near the commercially attractive region.

They also have high thermal stability, well-defined pore structure and high surface area. However, they have fragile structures, which make the formation of industrial-scale membranes difficult. In addition, inorganic membrane fabrication requires higher cost as they are more expensive than organic polymer membranes [43, 49].

2.4 Mixed Matrix Membranes for Gas Separation

As it was discussed in previous sections, the performance of polymer membranes are limited by a trade-off upper bound proposed by Robeson although they are easy to operate and suitable for many applications. On the other hand, inorganic membranes exhibit significantly higher separation performance but some problems such as being inherently brittle, low reproducibility and complicated fabrication procedures pose an obstacle on the industrial applications of them. These limitations of polymeric and inorganic membranes revealed the need for development of new membrane materials or new techniques to enhance the separation processes [7, 53, 54].

In 1970s, Paul and Kemp found that addition of zeolite 5A particles into a rubbery polymer polydimethyl siloxane (PDMS) considerably increased the diffusion time lag for CO_2 and CH_4, but had a minor effect on steady-state permeation. This was the first time MMMs were reported for gas separation. Then in mid-1980s, researchers at Universal Oil Products (UOP) firstly reported that composite polymer/adsorbent (zeolite) membranes show better separation performance compared to the corresponding pure polymeric membranes. They incorporated silicalite particles into the polymer cellulose acetate (CA) matrix and observed an enhanced O_2/N_2 separation performance [8, 54].

Recently, MMMs have been of great interest for researches as they are assumed to be promising candidates for exceeding the trade-off line. MMMs consist of an organic polymer phase (continuous phase) and inorganic particle phase (dispersed phase), as shown schematically in Figure 2.6. These composite membranes combine the low cost and processability of polymer membranes with superior permeability and selectivity of inorganic membranes. In other words, they potentially provide a solution both to the trade-off issues of the polymeric membranes and to the high cost and inherent fragility problems of inorganic membranes. While continuous phase is

typically a polymer; dispersed phase may be zeolite, carbon molecular sieves (CMS) or nano-sized particles [7, 8, 13, 53].

Figure 2.6 : Schematic representation of a MMM.

There are several models used to determine the separation performance of MMMs. First one was derived by Maxwell in 1870s for the evaluation of the dielectric properties of composite materials. This so-called Maxwell model has been accepted and widely used for estimating permeability and selectivity of MMMs, particularly the ones containing low amounts of inorganic particles. Maxwell model was developed assuming ideal morphology that there are no defective voids in polymer/inorganic particle interphase At low loadings of inorganic particles, the permeation of gas molecules takes place by combination of diffusion through the polymer matrix and through the pores of filler particles dispersed in polymer phase. The effective permeability of a MMM including a dilute suspension of spherical inorganic particles can be calculated by Equation **2.9**, which is the well-known Maxwell equation

$$P = P_c \left[\frac{P_d + 2P_c - 2\varphi(P_c - P_d)}{P_d + 2P_c + \varphi(P_c - P_d)} \right]$$
(2.9)

where P is the overall permeability of the MMM, P_c is the permeability of the continuous (polymer) phase, P_d is the permeability of the dispersed (inorganic) phase and φ is the volume fraction of the dispersed phase [8, 13, 54].

As seen on Figure 2.7, individual inorganic particles are considered to be well dispersed and separated from each other in the polymer matrix. In this case, one inorganic particle is only in contact with one or two other particles and the average permeability increases moderately according to the above Maxwell equation. However, the situation is different at particle loadings above the percolation threshold, which is a critical value where inorganic particles form continuous channels within the membrane and almost all particles attached to the channels. This

critical loading value is considered to be about 30 volume percent. Above the percolation threshold, permeation of gases takes place through two interpenetrated continuous phases. At very high inorganic particle loadings, polymer phase is assumed to become the dispersed phase, so the continuous and dispersed phases reverse in the Maxwell model [13].
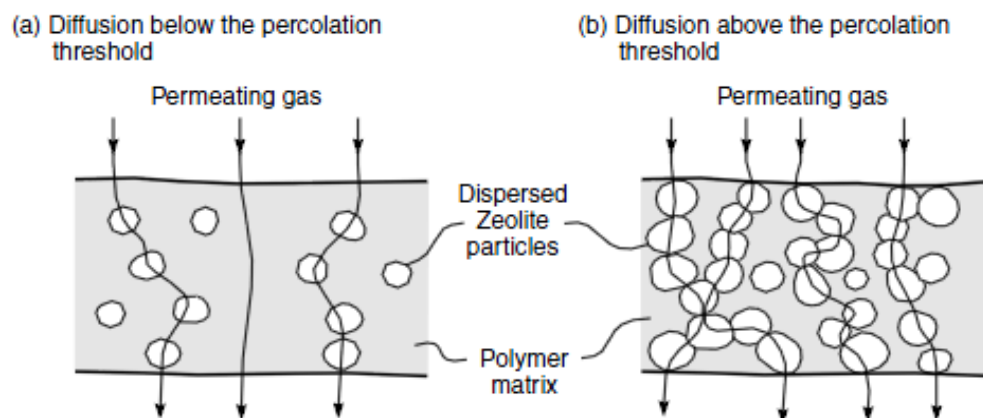
Figure 2.7 : Schematic representation of gas permeation through MMMs containing (a) low loadings, (b) high loadings of zeolite particles [13].

Conventionally zeolites, carbon molecular sieves (CMSs) and silica nanoparticles have been used as dispersed phase in MMM fabrication [7]. There are numerous studies in the literature carried out about the gas separation performance of MMMs comprising these conventional fillers dispersed in different polymer materials. Table 2.3 summarizes practically some of the reported CH_4/CO_2 separation properties of these MMMs.

Although conventional fillers have been widely used in MMM formation, the preparation of defect-free flat dense membranes requires some special techniques and treatment. One of the problems reported is the agglomeration of inorganic particles during the MMM solution preparation. In this case, mixing techniques are applied to break up particle agglomerates. Another problem is the partial incompatibility between polymer and inorganic particle that causes voids at the polymer/filler interface. This problem mostly takes place in glassy polymers having poor polymer chain mobility. It results in a weak interaction between the polymer matrix and filler particles and growth of undesirable channels between two phases. Gas molecules bypass these non-selective voids so the selectivity weakens at the end. Several techniques have been used to avoid the formation of these defects at the interface. One of them is to embed low molecular-weight additives (LMWA) to film

solution, which act as compatibilizer. Silane-coupling agents have been also used for modification of filler's external surface and promoting adhesion between the polymer and filler particles. Annealing above the glass transition temperature (T_g) also improves the adhesion between polymer and filler particles by eliminating the stress generated during solvent evaporation. Priming is also used as a technique to enhance the adhesion between polymer and filler, which is coating of filler particles with a thin layer of polymer before incorporating them into the bulk polymer [7, 55].

Table 2.3 : Comparison of various pure polymer and MMM single gas permeabilities and ideal selectivities of CO_2/CH_4 at 35ºC.

Polymer matrix	Filler (loading)	Additive (loading)	Pure polymer		MMM		Ref.
			P_{CO_2} [a]	α_{CO_2/CH_4} [b]	P_{CO_2}	α_{CO_2/CH_4}	
PES[c]	SAPO-34 (20 wt %)	-	4.45	33.2	5.77	37.0	[55]
		HMA (4 wt %)			2.07	40.6	
		HMA (10 wt %)			1.34	44.7	
P84 PI[d]	Zeolite 4A (20 wt %)	-	5.72	6.6	4.62	6.7	[56]
	Zeolite 13X (20 wt %)	-			5.28	6.2	
	Zeolite 13X (20 wt %)	-			11.22	25.1	
PS[e]	MCM-41 (20 wt %)	-	4.50	26.5	7.80	23.0	[57]
PC[f]	Zeolite 4A (20 wt %)	pNA (wt %)	8.80	23.5	3.97	51.0	[58]
Matrimid® 5218	Meso ZSM-5 (20 wt %)	-	7.29	34.7	8.65	66.1	[59]
CA[g]	Silicalite-1 (25 wt %)	-	11	41.0	18	40.0	[60]
Matrimid® 5218	CMS[h] (19 vol %)	-	10	35.3	10.60	46.7	[61]
	CMS (36 vol %)	-			12.60	68.6	
Ultem® 1000	CMS (16 vol %)	-	1.45	38.8	2.51	43.0	[61]
	CMS (35 vol %)	-			4.48	53.7	

[a] Permeability of CO_2, 1 Barrer = 10^{-10} cm^3(STP)·cm/cm^2·s·cmHg

[b] Permselectivity of CO_2 to CH_4

[c] PES: Polyethersulfone,   [d] PI: Polyimide,   [e] PS: Polysulfone

[f] PC: Polycarbonate,   [g] CA: Cellulose acetate

The gas separation performance of MMMs varies in a wide range as it is affected by many different factors, as can be seen in Table 2.3. The preparation technique, the zeolite-loading amount, the convenience of both polymer and inorganic material for separation of the specific gas pair and some other parameters are effective on the performance of MMMs [56].

Although the sieving characteristics of some conventional fillers such as zeolites, silica and CMS are suitable for separating particular gas pairs, there are still some issues needed to be overcome meeting the expectations for industrial applications. As mentioned before, the zeolite/polymer interface incompatibility is one of the most important problems that leads to poor gas separation performance. Therefore, several researches have been done about the usage of promising alternative materials. Some of these emerging materials are carbon nanotubes, clay and metal organic frameworks (MOFs) [7, 62].

2.5 MOF-Containing Mixed Matrix Membranes

Metal organic frameworks (MOFs) are a novel class of hybrid materials consisting of metal clusters bridged by organic linkers to create nanoporous structures. They are also named as coordination polymers [24, 62]. Li et al. first reported MOF synthesis in 1999 for MOF-5 crystals [63]. Afterwards, several thousand MOF materials have been synthesized [62]. Figure 2.8 illustrates some MOF types having different frameworks and porosities.

As they have high surface area, high thermal and chemical stability, tunable pore volume and chemical properties, MOFs are seen as attractive materials for several applications such as gas separation membranes, selective gas adsorption, hydrogen storage, etc. Utilization of MOFs as dispersed phase in a mixed matrix membrane (MMM) has become an attractive research area. The organic linkers in MOFs have affinity to polymer chains so the control of MOF/polymer interface is easier than zeolite/polymer interface. Defect-free MMMs can be fabricated with MOF particles without any modification through surface treatment unlike zeolites. Another important advantage of MOFs over zeolites is that numerous MOFs can be synthesized with different pore sizes and functionalities by changing the combination of metal and organic linker. Furthermore, MOFs have higher pore volume and lower

density than zeolites. These unique characteristics make the usage of MOFs more advantageous than zeolites in composite membrane preparation [25, 30, 62].
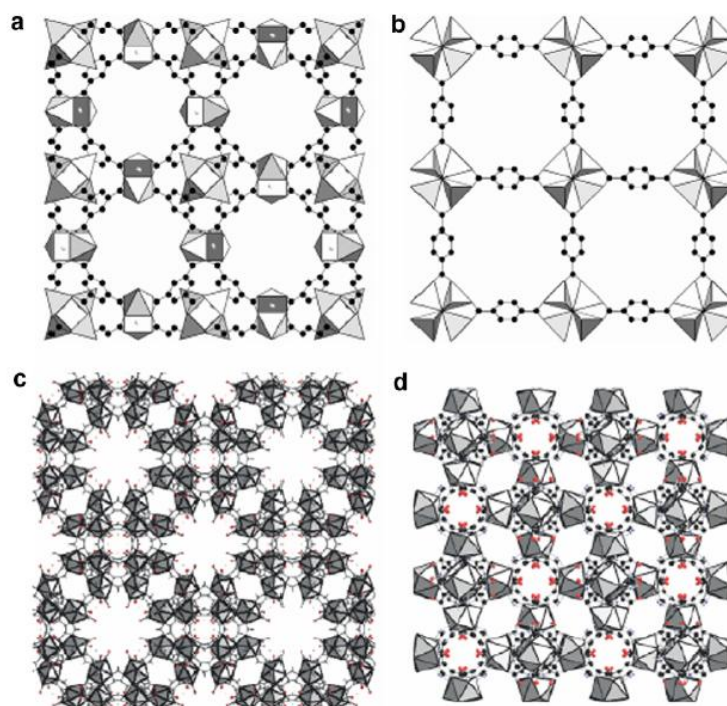
Figure 2.8 : A few MOF types with different forms of frameworks and porosity : (a) HKUST-1, (b) MOF-5, (c) *Sod*-ZMOF, (d) *Rho*-ZMOF [7].

The MOF containing MMMs were first explored by Yehia and co-workers in 2004 [64]. They incorporated copper(II) biphenyl dicarboxylate-triethylenediamine in poly(3-acetoxyethylthiophene) for the fabrication of MMM and obtained improvements in CH_4 selectivity compared to neat polymer membrane [53, 64]. Zeolitic imidazolate frameworks (ZIFs) were then introduced as a subclass of MOFs whose frameworks resemble the framework of zeolites. ZIFs also have exceptionally high thermal and chemical stability, very high surface area and microporosity that make them ideal candidates for gas separation applications [30]. Researches indicated that some ZIF types could be described as attractive molecular sieves for small gas molecules such as CO_2 and H_2 [62, 65, 66].

Recently, several MOF containing MMMs have been reported investigating the gas separation performance for different types of MOF or ZIF materials. Table 2.4 gives a brief literature review about the reported CH_4/CO_2 separation properties of these MMMs.

Table 2.4 : Comparison of various pure polymer and MOF containing MMM single gas permeabilities and ideal selectivities for CO_2/CH_4 at 35°C.

Polymer matrix	Filler	Loading	Pure polymer		MMM		Ref.
			P_{CO_2} [a]	α_{CO_2/CH_4} [b]	P_{CO_2}	α_{CO_2/CH_4}	
Matrimid	MOF-5	10 wt % 20 wt % 30 wt %	9	41	11.1 13.8 20.2	51.0 40.5 44.7	[53]
Matrimid	Cu-BPY-HFS [c]	10 wt % 20 wt % 30 wt % 40 wt %	7.29	34.71	7.81 9.88 10.36 15.06	31.9 27.6 27.4 25.6	[9]
PVAc [d]	CuTPA [e]	15 wt %	2.44	34.9	3.26	40.4	[67]
PS	Cu$_3$(BTC)$_2$ [f]	5 wt % 10 wt %	6.54	18.5	7.55 7.93	21.5 7.4	[68]
Matrimid	ZIF-8	20 wt % 30 wt % 40 wt % 50 wt % 60 wt %	9.52	39.7	9.08 14.20 24.55 4.54 7.89	50.4 38.7 28.6 126 82.4	[66]
Ultem	ZIF-90A [g]	15 wt %	1.45	38.5	1.98	39.5	[62]
Matrimid	ZIF-90A	15 wt %	7.80	35	10.2	35	[62]
6FDA-DAM	ZIF-90A ZIF-90B [h]	15 wt % 15 wt %	390	24	720 590	37 34	[62]

[a] Permeability of CO_2, 1 Barrer = 10^{-10} cm^3(STP)·cm/cm^2·s·cmHg

[b] Permselectivity of CO_2 to CH_4

[c] Cu-BPY-HFS: Cu-4,4'-bipyridine–hexafluorosilicate

[d] PVAc: Polyvinyl acetate,   [e] CuTPA: a MOF of copper and terephthalic acid

[f] Cu$_3$(BTC)$_2$: Copper (II)-benzene-1,3,5-tricarboxylate

[g] ZIF-90A: ZIF-90 particles formed in DMF/methanol mixture

[g] ZIF-90B: ZIF-90 particles formed in DMF/water mixture

As also seen in Table 2.4, several studies have shown that MOFs are very promising candidates for selective gas separation due to their superior selectivity and tunable properties [7]. Although some MOF materials were incorporated into polymer matrices and investigated for separation of particular gas pairs, there are still many types waiting for investigation.

3. MATERIALS AND EXPERIMENTAL PROCEDURES

In mixed matrix membrane fabrication, many different types of polymer/filler combinations and preparation methods can be used to obtain highly selective MMMs for the specific component in a gas mixture.

This section firstly presents the criteria to determine suitable materials for the introduced purpose. After that, the experimental procedures both for synthesis and ion-exchange of MOF crystals, and preparation of MMMs are explained. Finally, the characterization techniques for MOF particles and membranes are reported.

3.1 Material Selection

In MMM preparation, material selection for both the continuous phase (polymer matrix) and the dispersed phase (inorganic or inorganic-organic hybrid material) are key aspects. While the polymer material basically determines the minimum performance of the resultant MMM, the addition of appropriately selected dispersed particles may improve the separation performance by preferentially passing the desired component(s) if defect-free membranes could be obtained [69].

3.1.1 Polymer selection
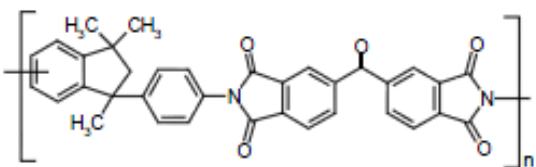
A variety of polymer materials such as cellulose acetate, polysulfones, polycarbonates and polyimides have been commonly used for commercial gas separations. For natural gas purification (CO_2, H_2S, H_2O removal), glassy polymeric membranes have been widely preferred [23, 66]. As mentioned before, glassy polymers favor the permeation of smaller molecules because the decrease in diffusion coefficients with increasing permeate size is relatively higher in glassy materials compared to rubbers. Therefore, when used to separate CO_2 from a CH_4/CO_2 gas pair, glassy polymers preferentially permeate CO_2 [13, 16]. Among other glassy polymers, polyimide materials are particularly attractive as they have high thermal, mechanical and chemical resistance as well as having high

permeability and selectivity values. They are assumed to endure high-pressure natural gas feeds due to their strong mechanical properties [23, 66].

Matrimid is a commercially available polyimide that has a relatively higher gas separation performance for CH_4/CO_2 gas pair compared to other polyimides [25, 70]. It also has high T_g and good processability [71]. According to the previous studies [9, 53, 72, 73], its CO_2/CH_4 ideal selectivity has been reported as approximately between 35 and 41 at low or moderate pressures and at 35ºC temperature. There are also several studies that different MOF particles incorporated into Matrimid polymer matrix and CO_2/CH_4 separation performance successfully enhanced [9, 53, 62]. These studies indicate that Matrimid polyimide has a promising background about natural gas purification and highly selective MMMs could be developed with other MOF materials that have not been studied yet.

Consequently, commercially available Matrimid® 5218, which consists of 3,3',4,4'-benzophenone tetracarboxylic dianhydride and diamiophenylindane monomers, was chosen in this study as the polymer material for preparing membranes. It is soluble in many common organic solvents such as N-methylpyrolidone (NMP), N,N'-dimethyl formamide (DMF), N,N',dimethylacetamide (DMAc) and chloroform [59, 74]. The chemical structure and physical properties of Matrimid® 5218 are indicated in Table 3.1. Matrimid® 5218 was purchased from Huntsman Advanced Materials Americas Inc.

Table 3.1 : Chemical structure and physical properties of Matrimid® 5218 [72, 75].

Polymer	Chemical Structure	Density (g/cm^3)	T_g (ºC)
Matrimid® 5218		1.23	308

3.1.2 MOF selection

Selecting the appropriate filler material improves the separation performance of MMMs compared to the corresponding pure polymer membrane, in the absence of interfacial defects. The chemical structure, surface characteristics, particle size distribution and aspect ratio of the filler material are assumed to be very crucial for

the performance of resultant MMMs [69, 76]. While using conventional fillers such as zeolite, silica and activated carbons, one of the most important problems is non-selective voids formed at the filler/polymer interface due to poor compatibilities of two phases. Some recent studies propose that preparation of defect-free MMMs is relatively easy when MOFs are used as filler rather than traditional inorganic fillers. This superiority is attributed to the partially organic structure of MOF materials, which increases their interaction with the polymer bulk material. By this way, the formation of undesired micro-gaps at the interface could be prevented [25, 66, 76].

While using MOFs as dispersed particles in MMMs, selecting the appropriate MOF type to achieve desired separation performance is a challenge because there are thousands of MOFs that could potentially be used [25, 77]. As mentioned in section 2.5, multiple MOFs have been investigated as fillers in MMMs [9, 53, 65-68]. However, there are still many which have not been explored yet. Zeolite-like metal organic frameworks (ZMOFs) can be regarded as one type of them. Although several gas adsorption studies about ZMOFs were carried out before [78-80], no MMM studies have been performed using these materials as the dispersed phase.

ZMOFs are a novel subclass of MOFs possessing anionic framework unlike other MOFs and ZIFs which typically have neutral framework. They have framework topologies resembling zeolites; transition metals replace Si or Al atoms and organic linkers (imidazolate units, symbolized as IM) replace oxygen bridges (e.g. -Si-O-Si-) in zeolites [78, 80, 81]. A schematical depiction of similarities between zeolites and ZMOFs/ZIFs is illustrated in Figure 3.1.
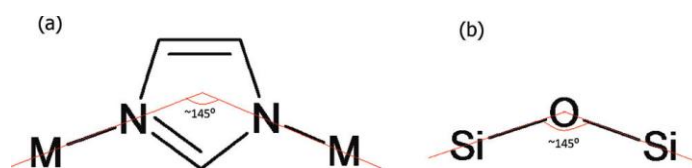
Figure 3.1 : The bridging angles in (a) ZMOFs/ZIFs and (b) zeolites [82]

The charge-compensating extra-framework cations exist in the pores of ZMOF structures which increase the interactions with guest molecules and improve their gas separation, gas storage and ion-exchange capability. The ion-exchange process is assumed to change the binding energy of adsorbate molecules to the ZMOF structure as it changes the electron density in the pores of ZMOF. Hence, ZMOFs have a

potential to be optimized for any specific gas molecule(s). ZMOFs are also reported to be stable in the presence of water, while most of the MOFs are unstable [79, 80].

In this work, *sod*-ZMOF was chosen as filler material using in MMMs. It represents the first example of MOFs with sodalite topology which has anionic framework. Metal ion source of *sod*-ZMOF is indium (III) and bridging linker is double deprotonated 4,5-imidazoledicarboxylic acid (H_3ImDC). It has micropores whose diameters are approximately 9.6 Å. The crystal structure of *sod*-ZMOF is demonstrated in Figure 3.2. The negatively charged framework of *sod*-ZMOF is charge-compensated by imidazolium cations which can easily be ion-exchanged with alkali metal ions.
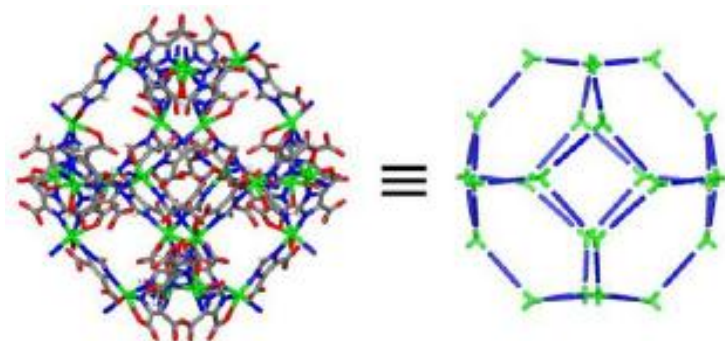
Figure 3.2 : A fragment of the *sod*-ZMOF crystal [83].

Sod-ZMOF is also insoluble in water and common organic solvents, and has very high thermal, chemical and mechanical stability. Calleja et al. [79] followed the thermal stability of *sod*-ZMOF crystals by XRD and the patterns showed that their crystallinity begins to disappear at 250 °C, as it can be seen on Figure 3.3.
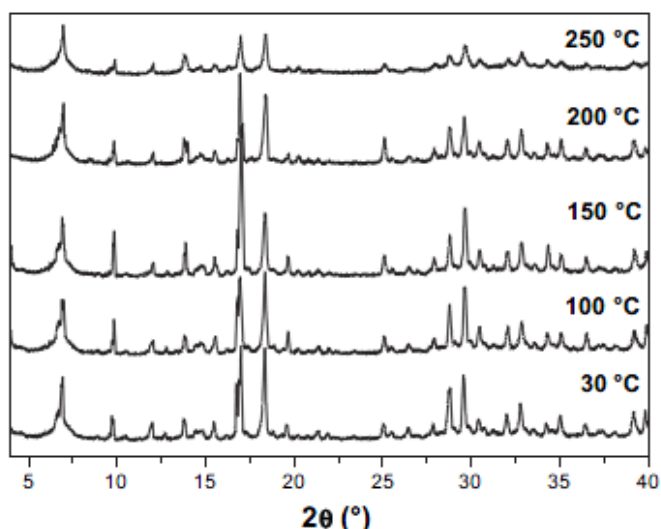
Figure 3.3 : Experimental XRD patterns of as-synthesized *sod*-ZMOF material at different temperatures [79].

26

This study proved the structural stability of *sod*-ZMOF material, which was also a criterion while choosing the appropriate ZMOF type for MMM preparation. When it was compared with *rho*-ZMOF, which is another ZMOF material having rhombic topology, *sod*-ZMOF was reported as thermally and chemically more stable [80, 83, 84].

In another study performed by Chen et al. [80], CO_2 adsorption isotherms of ZIF-8 and ZMOF samples were obtained and they were compared with each other. ZIF-8 was a good choice for comparison as it is a widely investigated ZIF material having the same sodalite topology as *sod*-ZMOF. Table 3.2 summarizes the textural properties and CO_2 capture capacities of these materials. Figure 3.3 also presents the CO_2 and N_2 adsorption-desorption isotherms of *sod*-ZMOF and ZIF-8 particles at 25 ºC temperature. As can be seen in the table, *sod*-ZMOF exhibits much higher adsorption capacity than ZIF-8, even its surface area is considerably smaller. This superior performance was attributed to the charged structure of ZMOF materials. The charge-compensating extraframework cations in the cavities of ZMOF interact with adsorbate molecules having quadrupoles (e.g. CO_2) and generate new adsorption sites for these molecules [80]. This study was also effective for choosing *sod*-ZMOF as a filler material to test whether the proven high affinity for CO_2 would also enhance the separation performance of polymer membranes or not.

Table 3.2 : Textural properties and CO_2 capture capacities of ZMOF and ZIF-8 samples [80].

Sample	S_{BET} (m^2/g)[a]	V_{pore} (cm^3/g)[b]	CO_2 uptake (mg/g)[c]
ZIF-8	1450	0.50	30
Sod-ZMOF	375	0.16	53
Li^+-*sod*-ZMOF*	345	0.16	54
Na^+-*sod*-ZMOF*	373	0.17	56
K^+-*sod*-ZMOF*	363	0.16	61

[a] S_{BET}: BET surface area of the sample
[b] V_{pore} : Pore volume of the sample
[c] CO_2 uptake (mg/g) measured at 1 bar pressure.
* *sod*-ZMOF particles ion-exchanged with lithium (Li^+), sodium (Na^+) and potassium (K^+) cations.
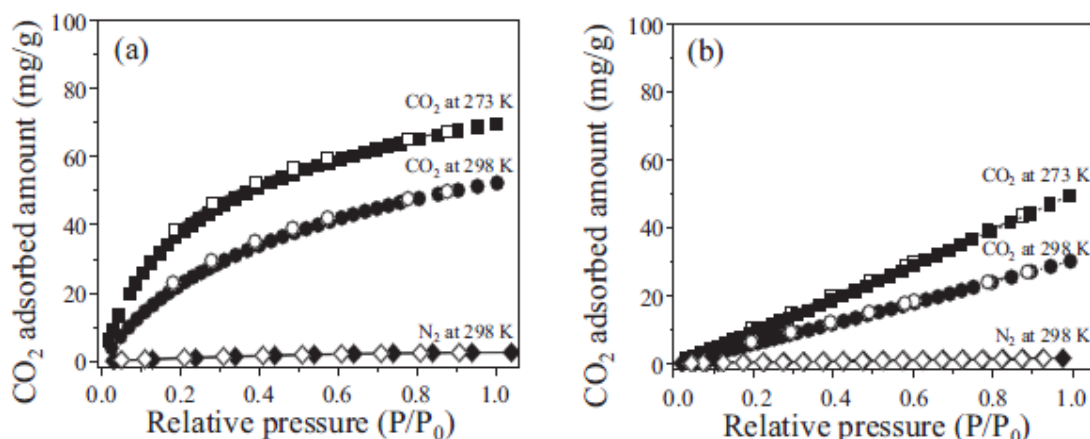
Figure 3.4 : CO_2 and N_2 adsorption-desorption isotherms of (a) sod-ZMOF, and (b) ZIF-8 [80].

3.2 *Sod*-ZMOF Synthesis and Ion-Exchange Procedure

Sod-ZMOF was synthesized with classical solvothermal method following the procedure published in literature [79, 84]. The purities and suppliers of the chemicals used for *sod*-ZMOF synthesis are summarized in Table 3.3.

Table 3.3 : The list of materials used for *sod*-ZMOF synthesis

Material	Purity	Supplier
4,5-Imidazoledicarboxylic acid (H_3ImDC)	97 %	Sigma-Aldrich
Indium nitrate ($In(NO_3)_3 \cdot XH_2O$)	99.9 %	Sigma-Aldrich
Dimethylformamide (DMF)	≥ 99.8 %	Merck
Acetonitrile (CH_3CN)	≥ 99.9 %	Merck
Imidazole (Im)	≥ 99 %	Sigma-Aldrich
Nitric acid (HNO_3)	65 %	Carlo Erba

4,5-Imidazoledicarboxylic acid (H_3ImDC), indium nitrate ($In(NO_3)_3 \cdot XH_2O$), dimethylformamide (DMF), acetonitrile (CH_3CN), imidazole (Im) and nitric acid (HNO_3); (with 1 In:3 H_3ImDC:6.9 Im:24 HNO_3:446 DMF:220 CH_3CN molar ratio) were respectively added into a vial and stirred for an hour. After mixing well, the milky dispersion was heated up to 85ºC for 12 h and then up to 105 ºC for 23 h in an oven. The first step is nucleation time (t_n) and the second step is crystallization time (t_c). After the reaction was completed at solvothermal conditions, colorless polyhedral crystals were collected by filtration, washed with methanol to remove the remaining DMF from the surface and pores of the MOF material, and air-dried at

room temperature. The obtained crystals had a particle size between 50-200 μm, as reported in the literature [79, 80]. Nevertheless, the particles must be smaller for incorporating into a polymer matrix and preparing MMMs, so different studies were performed by changing the synthesis conditions (synthesis temperature/time, pH of the reaction medium, etc.) for particle size reduction. By using one-half of the nitric acid used before, the smaller particles were obtained which could be assumed to be suitable for MMM preparation.

Sod-ZMOF was further ion-exchanged with a standard ion-exchange procedure [79-80]: 0.1 M NaCl solution was prepared and *sod*-ZMOF crystals were stirred in this mixture for 24 h at room temperature. The ion-exchange process was repeated 4 times, refreshing the solution every day. Ion-exchanged *sod*-ZMOF materials are named as Na^+-*sod*-ZMOF.

3.3 Membrane Preparation

The procedure for flat dense membrane preparation can briefly be described with following steps:

- ➢ Preparation of homogeneous polymer/(filler)/solvent film solution,

- ➢ Casting the solution on a smooth surface (glass, mirror, etc.),

- ➢ Evaporation of the solvent,

- ➢ Annealing at high temperatures for removal of the residual solvent.

This procedure may both be used for pure polymeric and mixed matrix membrane formation. Nevertheless, the details in these procedures may also vary in a wide range for MMMs as they depend on the polymers, solvents and fillers used [8].

3.3.1 Pure polymer membranes

In this work, pure polymer membranes were fabricated to use as the reference when interpreting the effect of fillers loaded in MMMs. Pure polymer membranes were prepared by dissolving a certain amount of Matrimid in DMF solvent. Matrimid® 5218 was placed in a vacuum oven at 120 ºC and dried overnight under active vacuum prior to use in membrane formation. Dense membranes were prepared from a DMF solution containing 15 wt% Matrimid. The conventional solution-casting technique was used. A particular amount of Matrimid and required DMF was

weighed and the Matrimid was added into the solvent periodically (with 2-hour intervals) in 5 equal portions to have an effective solvation. After the total amount of polymer was added and dissolved, the film solution was stirred overnight on a magnetic stirrer. Then, the stirring was stopped and the film solution was poured on a smooth mirror surface after waiting for about half an hour to minimize air bubbles in the solution. The steps for preparing flat dense films are itemized as follows:

- Membranes were cast in a laminar flow hood onto a mirror substrate using a film casting knife and table, having 500 μm initial thickness, for obtaining a flat membrane.

- The film then quickly placed in an oven at 80 ºC for three hours and after solvent evaporation, it was peeled off from the mirror surface.

- It was placed in the oven again and kept at 100ºC overnight.

- Then it was heated to 200ºC with 1ºC/min heating rate and further annealed at this temperature for 48 h under vacuum to completely remove the residual solvent.

- It was cooled down to room temperature inside the oven naturally and further stored in a desiccator.

The average membrane thickness was 35 μm after annealing.

3.3.2 Mixed matrix membranes

In this study, *sod*-ZMOF particles were used for the first time as fillers in MMM fabrication, therefore there is not an applicable preparation technique published in literature specific for this MOF type. The previously reported preparation methods [53, 76, 85] for some other MOF particles were used to develop a convenient method. Prior to membrane preparation, both Matrimid® 5218 and *sod*-ZMOF were dried overnight at 120°C under vacuum. Dense MMMs containing 5 and 10 wt% *sod*-ZMOF were prepared.

According to the determined loading, a particular amount of *sod*-ZMOF was dispersed in DMF. The suspension was stirred overnight on a magnetic stirrer. Then, the mixture was bath sonicated for 30 min to ensure a well dispersion before the required quantity of Matrimid (with a 15/85 Matrimid/solvent ratio) was added. Matrimid was again added into the dispersion periodically (with 2-hour intervals) in

5 equal portions. After the total amount of polymer powder was added, the whole mixture was allowed to stir for another night. Subsequently, the surface of a flat mirror was cleaned with ethanol and the film solution casted on it using a casting knife, having 800 μm initial thickness. Then the same heat treatment and annealing procedure (48 h at 200ºC) was applied as in pure polymer membrane. The thickness of dried MMMs varied from 45 to 65 μm. Figure 3.4 presents the general procedure appied for MMM preparation.
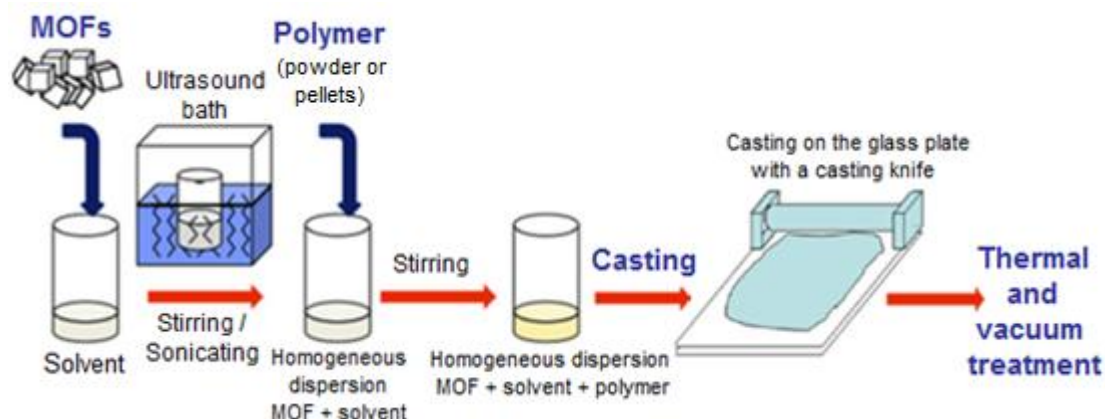
Figure 3.5 : General sheme for the preparation of MOF-containing MMMs.

3.4 Characterization Techniques

In this section, characterization techniques for both *sod*-ZMOF particles and membranes were presented. Firstly, structural and thermal properties of *sod*-ZMOF crystals were examined prior to preparation of MMMs. Then, standard characterization methods were applied to determine the membrane properties following the preparation of pure polymeric and mixed matrix membranes.

3.4.1 Characterization of *sod*-ZMOF crystals

Structural and morphological characterization of *sod*-ZMOF was made by X-ray diffraction (XRD) and scanning electron microscopy. Thermogravimetric analysis (TGA) was also used for thermal characterization of MOF particles.

3.4.1.1 X-ray diffraction

Powder X-ray diffraction (PXRD or XRD) is a powerful technique for characterizing materials based on their constituent crystal structures. It is a noncontact and nondestructive method. In this technique, any material is irradiated by a

monochromated X-ray beam. If the material has crystalline structure (containing repeated arrays of atoms), it generates unique diffraction peaks. These diffraction peaks are material-specific so they are named as fingerprint of material. By this way, XRD is very significant in materials science as it can uniquely identify the presence and composition of phases. In a typical XRD analysis, the diffracted intensities are measured as a function of diffraction angle 2θ and the orientation of the sample, where 2θ is the angle between the diffracted and incident X-rays. By using powder X-ray diffractogram, it is also possible to quantitively calculate the crystallinity of samples [86, 87].

In this study, XRD patterns for synthesized *sod*-ZMOF particles were obtained to compare with the ones reported in literature to investigate whether the synthesis was performed successfully or not. It was obtained on a Panalytical X'Pert PRO diffractometer using CuKα (λ=1.54 Å) radiation in the 2θ range between 5º and 50º.

3.4.1.2 Scanning electron microscopy

Scanning electron microscopy (SEM) is an instrument used for the purpose of detailed morphological characterization. It provides highly magnified images of the surface of materials. The resolution of the SEM can generally approach less than 1 nm and the magnification can be adjusted from about 10 times (x10) to more than 500000 times (x500000) [87, 88].

In this study, SEM analysis was carried out using a JEOL JSM-6390LV instrument. *Sod*-ZMOF particles were attached on a sample holder with an adhesive carbon foil and coated with platinum (Pt) for 1 min at 15 mA, in order to obtain conductivity. An Emitech K550X instrument was used for coating. Samples were then characterized under high vacuum and a potential difference of 10 kV, at magnifications between x100 and x3000.

3.4.1.3 Thermogravimetric analysis

Thermogravimetric analysis (TGA) is a thermal analysis technique which examines the mass change of the sample as a function of temperature. The thermal events causing change in the mass of the sample are not only melting, crystallization or glass transition, but also absorption, desorption, sublimation, vaporization, oxidation, reduction and decomposition. TGA is used to characterize the thermal stability and

decomposition of materials under controlled conditions, and also to examine the kinetics of the occurring physico-chemical processes taking place in the sample. The quantity of volatile components such as absorbed moisture, residual solvent, etc. can be detected using this analysis technique [89].

In this study, TGA analyses of *sod*-ZMOF particles were carried out with a Perkin-Elmer Diamond TG/DTA instrument. A small amount of powder was weighed and analyzed between 50ºC and 550ºC with a scanning rate of 4ºC/min under flowing air of 100 ml/min. The obtained thermogram was then used to determine the decomposition temperature and thermal stability of *sod*-ZMOF material.

3.4.2 Membrane Characterization

Membrane characterization was carried out using some analysis techniques such as SEM, TGA, and differential scanning calorimetry (DSC) and gas separation properties of them were further investigated by gas permeability measurements.

3.4.2.1 Morphological and thermal characterization

SEM was used to investigate the cross-sections of mixed matrix membranes in order to determine the adhesion between continuous and dispersed phases. The thickness of the membranes was also confirmed by SEM images. Prior to analysis with SEM, a small piece of membrane was cut out and broken by immersing in liquid nitrogen for a few minutes to obtain a cross-section. Then, the sample was placed on a sample holder with an adhesive carbon foil and coated with platinum for 90 seconds. Finally, the MMM samples were examined via SEM and the images of cross-sections were obtained under high vacuum and a potential difference of 10 kV, at magnifications varying between x1500 and x10000.

Thermal characterization of membranes were mainly performed by two common methods: TGA and DSC. The basic principles of TGA were previously summarized. The TGA analyses of membranes were also carried out between 50ºC and 550ºC, but they were heated with a scanning rate of 10ºC/min under flowing N_2 of 200 ml/min. The obtained thermogram was then used to determine the amount of moisture and residual solvent in the sample. The data was also used as guide while determining a program for DSC analyses.

Differential scanning calorymetry (DSC) is a widely used technique for determining glass transition, melting and crystallization temperatures as well as heat of fusion for polymeric materials. DSC is an instrument basically containing two heat sensitive plates in a furnace, with thermocouples attached to the base of these two holders. The sample is placed in a sealed pan and inserted in one of these plates, and an identical empty sealed pan is inserted in the other plate as reference. Then, the temperature difference between the sample and reference pans is measured as a function of temperature or time, under controlled temperature conditions. This temperature difference is proportional with the change in heat flux. When the sample goes through a phase transformation, heat is absorbed or released and it causes a temperature difference between sample and reference. By this way, T_g of polymers is observed as a differential increase in the heat capacity of the sample due to the increase of molecular motion in the polymer [89, 90].

In this study, DSC measurements of membranes were performed with a Perkin-Elmer DSC-4000 instrument. A small amount of sample was weighed and placed in a standard alumina pan. After sealing, it was inserted into the DSC for analysis and a four-step heating sequence was applied. Firstly, the sample was heated from 30ºC to 310ºC with a heating rate of 20ºC/min, where 310ºC is slightly above the T_g of the polymer (Reported average T_g for Matrimid® 5218 was 308ºC). This heating step was applied because it is desired to erase the previous thermal history of a sample. Then, it was maintained at 310ºC for 5 min before cooling the sample to 250ºC with 30ºC/min rate. As a final step, the sample was re-heated from 250ºC to 400ºC with a heating rate of 10ºC/min. 400ºC is a temperature higher enough from the predicted T_g of the sample, so it is appropriate for seeing the glass transition obviously. This heating cycle was applied under inert N_2 atmosphere and T_g was calculated by half Cp extrapolation method.

3.4.2.2 Gas permeation measurements

The permeability measurements were performed with a constant volume-variable pressure permeation system. In this system, a pressure difference is created between two sides of the membrane, which was readily inserted in a permeation cell, and the gas permeation is provided towards the downstream chamber that has a constant volume. The gas stream accumulating at this calibrated volume leads to an increase

in pressure and the amount of permeate gas may be determined by following the pressure raise. Figure 3.5 presents the schematic illustration of the system. As it also can be seen from the figure, the permeation system principally consists of a permeation cell, upstream and downstream transducers, data acquision system and a gas chromatogram (GC). Permeation cell includes two halves and tightly encloses the membrane between them. Upstream transducer measures the upstream (feed) pressure and downstream transducer measures the downstream (permeate) pressure. Data acquision system records the upstream and downstream pressures, which are required for calculating the permeability, every one minute. The GC is also used for measuring the composition of feed and permeate streams while mixed gas conditions exist.
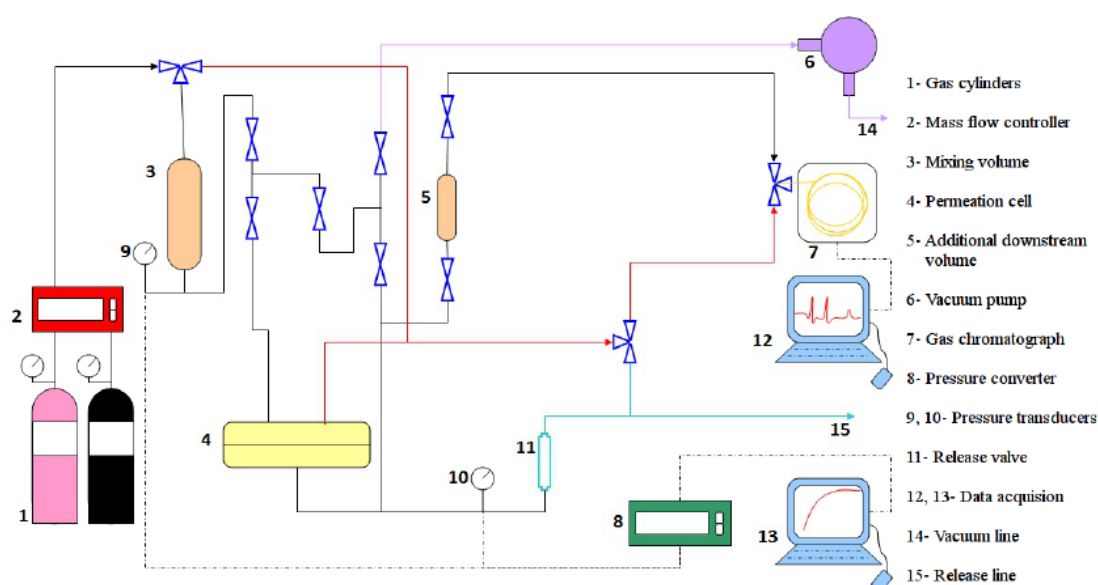
Figure 3.6 : Schematic depiction of the constant volume-variable pressure system used in this study.

Prior to be inserted into the permeation cell for permeation measurements, the membranes were immobilized by masking. For masking a membrane, a circle which has a smaller diameter from the membrane was cut out from an aluminum sheet and the membrane was attached on the adhesive side of the sheet. A same-size hole was also made on another smaller circle of aluminum sheet, which has a diameter slightly bigger than membrane. Then, the membrane was sandwiched between these two sheets and as a final step, the boundary between the membrane and the aluminum sheet on upstream side (reverse side of the aluminum sheet where membrane was attached) of the masked membrane was sealed with epoxy to avoid any leaks. The

membrane was ready for permeation measurements after the epoxy was completely hardened, which takes approximately 24 hours.

For gas permeation measurements, the masked membrane was attached to the lower half of the permeation cell and the upper half of the cell was placed onto it. Afterwards, the sealed cell was attached to the piping system through Swagelok® VCR fittings. Prior to feeding the gas to the upstream; the upstream and downstream sides were evacuated for 24 hours using a vacuum pump in order to remove residual solvent and any adsorbed gases in the membrane. Then, the gas was fed to the upstream after the valve connecting two sides of the membrane was closed. A time lag was observed in the first measurement. This means that it takes a certain time for gas molecules to fill the free volume of the membrane. After this time elapses, the membrane reaches steady-state and the rate of pressure increase in the downstream becomes linear. After each measurement, this rate of pressure increase (the slope of downstream pressure versus time) was calculated and it was repeated until the slope became almost constant for three following measurements.

The permeabilities were calculated from the pressure change vs. time at steady-state condition, by using Equation **3.2**

$$P_i = \frac{(\alpha_m - \alpha_l)Vl}{ART\Delta P} \tag{3.2}$$

where α_m is the rate of pressure increase in the downstream during measurement, α_l is the rate of leak in the downstream, V is the volume of the downstream side, l is the thickness of the membrane, A is the permeation area of the sample, R is the ideal gas constant, T is the temperature where the measurements were taken, and ΔP is the pressure difference between the upstream and the downstream.

In this study, all single gas measurements were carried out at 4000 mbar upstream pressure and 35ºC temperature. The downstream side was evacuated overnight prior to work with another gas stream in order to sweep away the gas molecules belonging to the previous feed stream.

4. RESULTS AND DISCUSSIONS

This chapter mainly consists of two parts. The first part presents the result for structural and thermal characterization of *sod*-ZMOF particles, and the second part gives the results for membranes and compares the properties of sod-ZMOF containing MMMs with pure Matrimid® 5218 membrane.

4.1 *Sod*-ZMOF Characterization

Sod-ZMOF crystals were obtained by following the reported solvothermal synthesis method [79, 84], so the resultant data obtained from characterization were also compared with the published ones.

Firstly, the particles were analyzed with X-ray diffraction. Figure 4.1 shows the XRD pattern of *sod*-ZMOF particles, both published [79] and synthesized in this study.
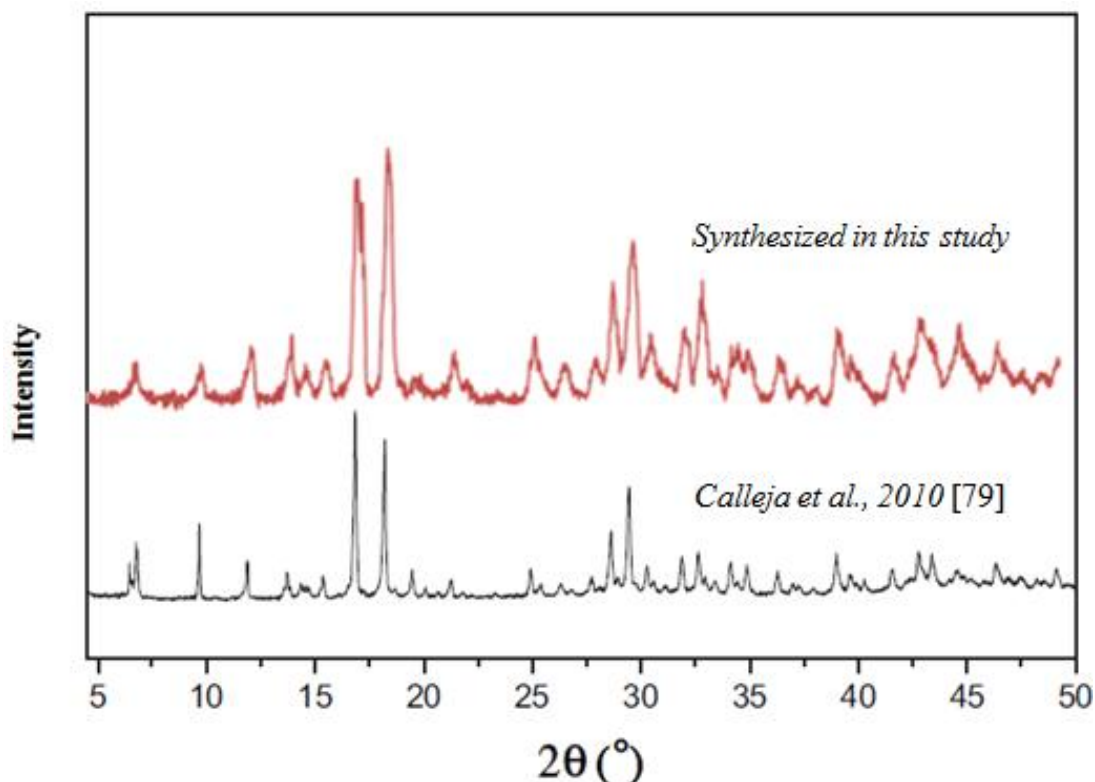
Figure 4.1 : Comparison of XRD patterns of *sod*-ZMOF crystals, synthesized in this study and the published one [79].

As it can be obviously seen on Figure 4.1, the XRD pattern of the *sod*-ZMOF crystals synthesized in this study was quite similar to the published one, which was synthesized with the same method [79]. It confirms that the *sod*-ZMOF particles were successfully synthesized.

Figure 4.2 presents the SEM images of the as-synthesized and Na^+ ion-exchanged *sod*-ZMOF particles. The images showed that as-synthesized *sod*-ZMOF samples were comprised of distinctly regular multi-faceted (tetrahedral) crystals. The SEM images showed the crystal particle size ranged from 2 μm to 20 μm for as-synthesized *sod*-ZMOF particles (Figures 4.2a and 4.2b).

On the other hand, Figures 4.2c and 4.2d indicates that the morphology of the *sod*-ZMOF crystals appeared to be substantially modified during the ion-exchange process. Nevertheless, the crystal structure did not collapse; as it was also confirmed by XRD patterns [79] showing the whole crystallinity were maintained during the ion-exchange procedure when pure methanol was used as the solvent medium.
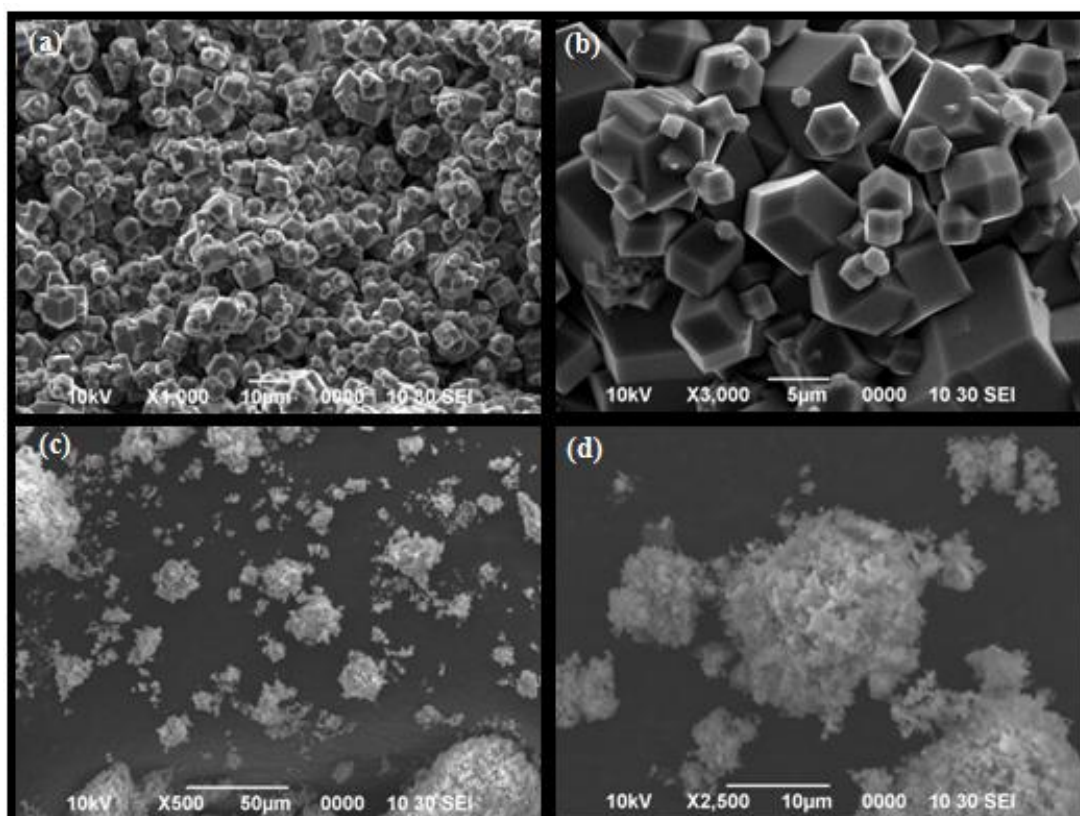
Figure 4.2 : SEM images of (a-b) as-synthesized, (c-d) Na^+-*sod*-ZMOF crystals.

In Figure 4.3, the TGA diagrams of both as-synthesized and ion-exchanged sod-ZMOF particles were presented. The thermogram for as-synthesized *sod*-ZMOF shows that there is not considerable weight loss until 200°C. Although the derivative thermogravimetric analysis (DTG) curve was not included in the figure for preventing complexity, there was a peak centered at 288°C, which was attributed to the degradation of structure-directing agent (SDA), imidazolium at about this temperature. As the thermal stability of ZMOFs are determined by the loss of SDAs, *sod*-ZMOFs could be said to remain thermally stable until about 290°C. In a recent study [79], it was illustrated by XRD patterns that the crystallinity of *sod*-ZMOF started to collapse at 250°C, as it was also indicated in the previous section (Figure 3.3). The next remarkable weight loss was seen at approximately 380°C, and this is related with the removal of organic linker of the framework. At this point, the crystal structure of the *sod*-ZMOF was assumed to be totally disappeared.
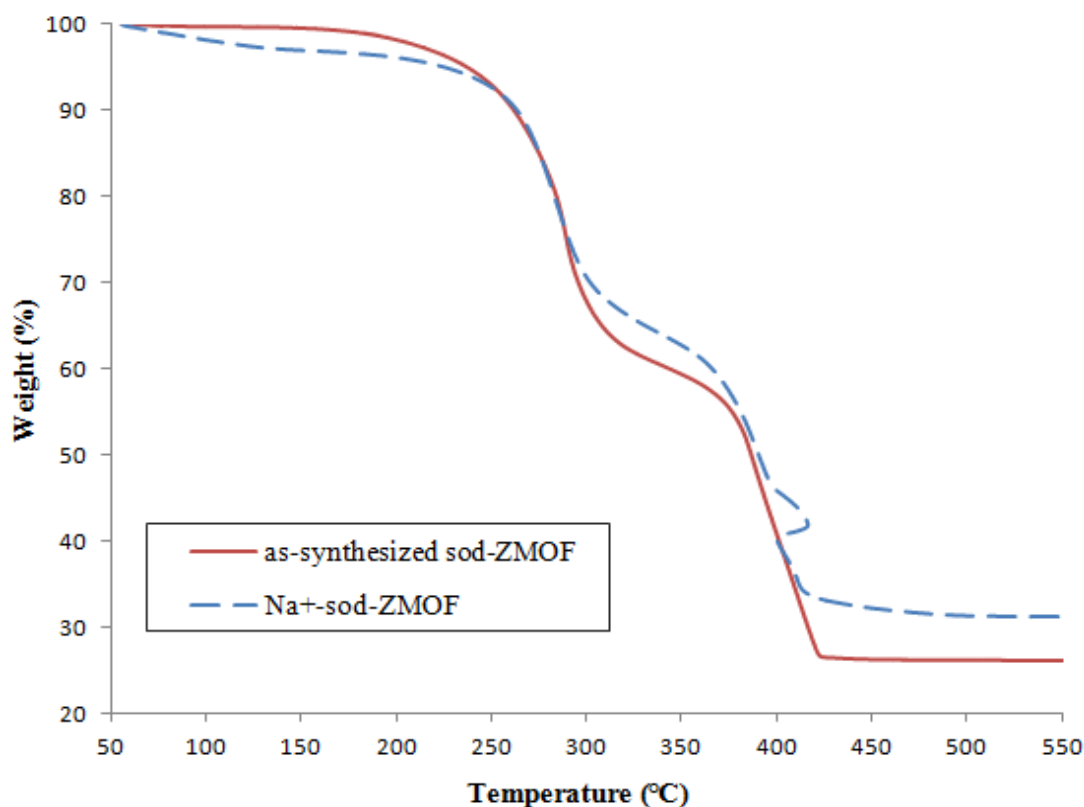
Figure 4.3 : TGA curves for as-synthesized and Na^{+}-*sod*-ZMOF crystals.

The cumulative weight losses at certain temperatures, starting from 50°C, were also indicated in Table 4.1. According to the table, the weight loss until reaching 153°C, which is the boiling point of DMF, was higher for ion-exchanged *sod*-ZMOF particles. This result can be described by having larger cavities after ion-exchange

process, as the organic imidazolium cations in the cavities were partially exchanged with smaller Na^+ ions. As a result, higher amount of solvent could be trapped in these larger cavities. On the other hand, total weight loss at the end of temperature scanning was smaller in ion-exchanged *sod*-ZMOF, this could also be explained by the increase in inorganic structure. Especially from 200°C to 300°C, there was a considerable difference (approximately 5%) in weight loss between two samples, as the organic SDA collapsed at this temperature interval and it was partially replaced by inorganic cations during ion-exchange.

Table 4.1 : Cumulative weight loss of *sod*-ZMOF particles, obtained from the TGA data.

Sample	Cumulative weight loss (%)					
	100°C	153°C	200°C	300°C	400°C	500°C
As-synthesized *sod*-ZMOF	0.42	0.60	1.91	32.08	59.11	73.77
Na^+- *sod*-ZMOF	1.79	3.02	3.82	29.19	54.07	68.70

4.2 Characterization of Membranes

For all membranes prepared in this study, morphological (SEM) and thermal (TGA, DSC) analysis as well as gas permeation measurements were performed.

4.2.1 Morphology

Figure 4.4 indicates the morphology of MMMs prepared by loading different amounts of both as-synthesized and ion-exchanged *sod*-ZMOF particles, obtained with SEM. The SEM images of *sod*-ZMOF/Matrimid membrane cross-sections showed good interfacial contact between *sod*-ZMOF crystals and polymer matrix, since there were no apparent voids at the polymer/filler interface. They also showed that there was a good particle distribution of *sod*-ZMOF particles in the continuous phase, as homogeneous morphologies were detected with virtually no agglomeration of MOF particles. These results signify that *sod*-ZMOF crystals showed excellent adhesion with the Matrimid® without any surface-compatibilization procedures and defect-free MMMs were obtained. Thus, these MMMs were considered to be promising candidates for enhanced gas permeation properties.
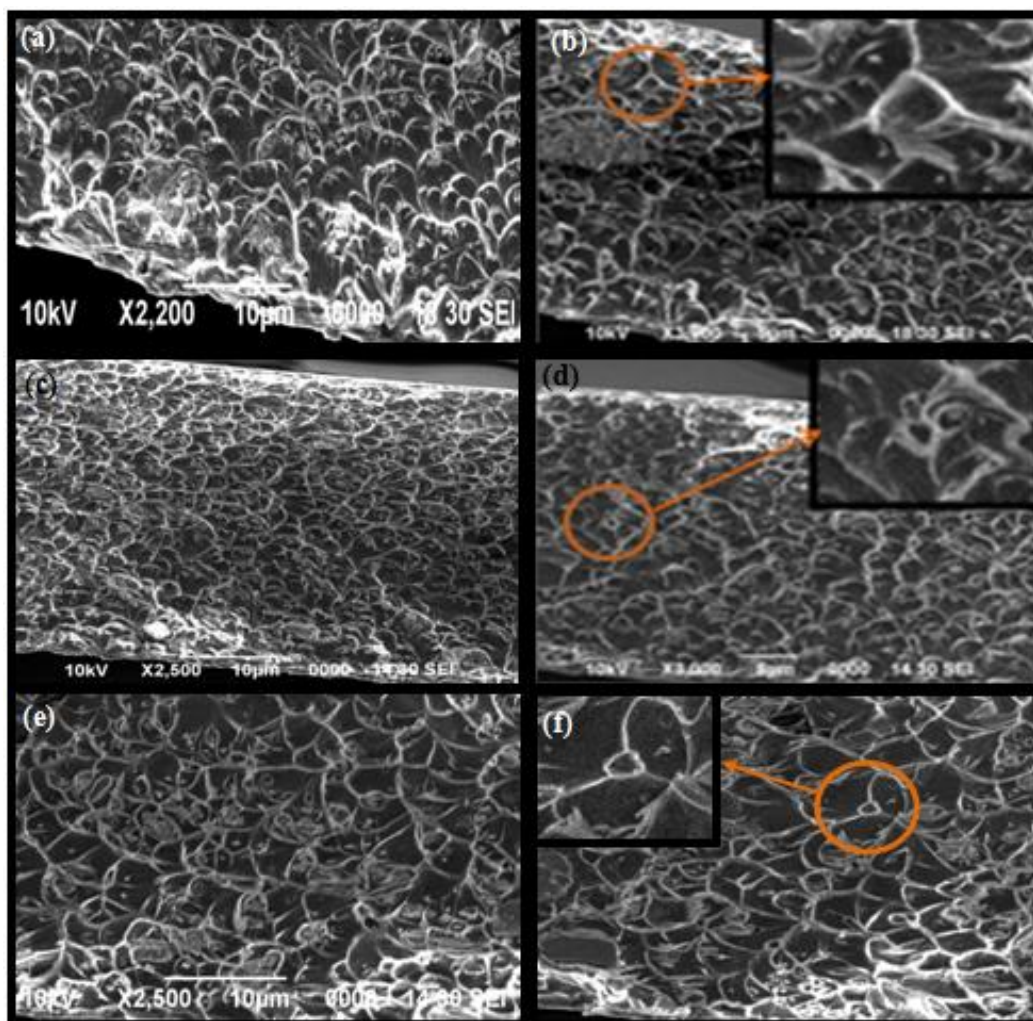
Figure 4.4 : SEM images of MMMs containing: (a-b) 5 wt% as-synthesized *sod*-ZMOF, (c-d) 10 wt% as-synthesized *sod*-ZMOF, (e-f) 10 wt% ion-exchanged *sod*-ZMOF particles.

The SEM images also showed that *sod*-ZMOF particles became smaller as they were incorporated into the polymer matrix to form MMMs, which was assumed to occur during mechanical stirring and sonicating processes.

In this study, it was also questioned whether these particles maintained their crystallinity after all mechanical and thermal treatments through MMM preparation or not. For this purpose, a MMM prepared containing 20% *sod*-ZMOF with the same procedure applied to the other membranes, and it was further analyzed with powder XRD. Figure 4.5b shows the XRD pattern of this MMM, in contrast to pure Matrimid® 5218 and as-synthesized *sod*-ZMOF crystals. According to the pattern obtained, there was no considerable loss in crystallinity of *sod*-ZMOF particles, only slight changes of some reflections. Thus, it can be said that the crystalline structure

of *sod*-ZMOF material was substantially conserved through the MMM preparation process.
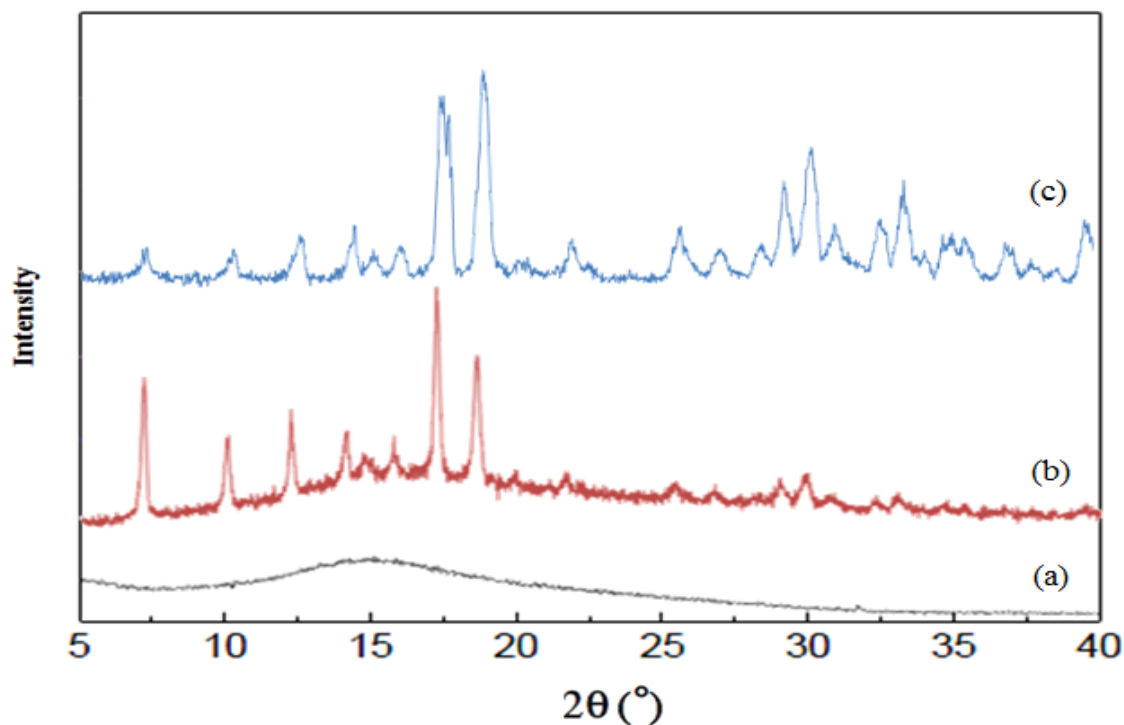
Figure 4.5 : XRD patterns of (a) pure Matrimid® 5218, (b) MMM containing 20 wt% *sod*-ZMOF, (c) as-synthesized *sod*-ZMOF particles.

4.2.2 Thermal properties

The membranes were investigated with TGA in order to determine the amount of moisture and residual solvent exist within the membrane. Figure 4.6 shows the TGA thermograms of mixed matrix membranes loaded with different amounts of (5 or 10 wt%) as-synthesized and Na$^+$-ion-exchanged *sod*-ZMOF particles. TGA curve of pure Matrimid® membrane was included for comparison. Table 4.2 also lists the cumulative weight loss in these samples. For both pure and *sod*-ZMOF containing Matrimid membranes, there was not considerable weight loss until the boiling point of DMF (153°C). This confirms that the removal of residual solvent as well as the adsorbed moisture was carried out successfully, with annealing the membranes at 200°C. Nevertheless, it must be noticed that the amount of residual solvent was higher in MMMs compared to the pure polymer membrane. This difference was attributed to the presence of *sod*-ZMOF particles having large cavities potentially entrapping more solvent at the interface. The weight losses between 300°C and 400°C were also relatively higher in MMMs, as the organic structure of *sod*-ZMOF

was totally lost at nearly 380°C. This was also confirmed quantitively by making a comparison between 5 wt% and 10 wt% *sod*-ZMOF containing MMMs: the weight loss at the temperature interval 300°C-400°C was 3.5% for 10% *sod*-ZMOF/Matrimid membrane while it was 1.77% for 5% *sod*-ZMOF/Matrimid membrane. In other words, the weight loss doubled in MMMs between 300°C and 400°C when the *sod*-ZMOF loading amount doubled, due to the lost of organic linkers in *sod*-ZMOF framework at this temperature interval.
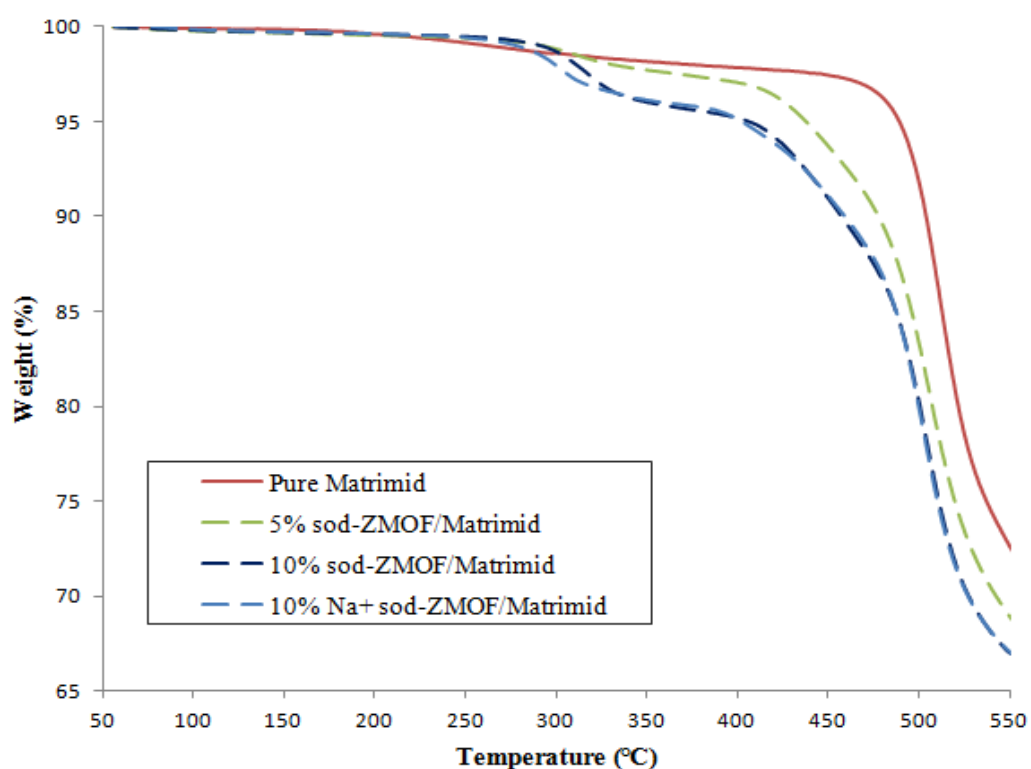
Figure 4.6 : TGA curves for pure and *sod*-ZMOF containing Matrimid membranes.

Table 4.2 : Cumulative weight loss of pure and *sod*-ZMOF containing Matrimid membranes, obtained from the TGA data.

Membrane	Cumulative weight loss (%)					
	100°C	153°C	200°C	300°C	400°C	500°C
Pure Matrimid® 5218	0.080	0.144	0.382	1.377	2.148	8.04
5% *sod*-ZMOF/Matrimid	0.211	0.320	0.449	1.172	2.944	16.84
10% *sod*-ZMOF/Matrimid	0.174	0.298	0.366	1.296	4.796	19.62
10% Na^+-*sod*-ZMOF/Matrimid	0.167	0.316	0.410	2.088	4.910	20.22

Figure 4.7 presents the DSC thermograms for MMMs. As the average T_g value for pure Matrimid® 5218 membrane was about 310°C, the T_g increased slightly with *sod*-ZMOF loading. These small increases could be a result of chain rigidification, which takes place when polymer chains in direct contact with MOF surface rigidify compared to the bulk polymer chains and form higher-T_g regions within the membrane. However, the increase of T_g values were not further interpreted as they were also falling within the experimental error.
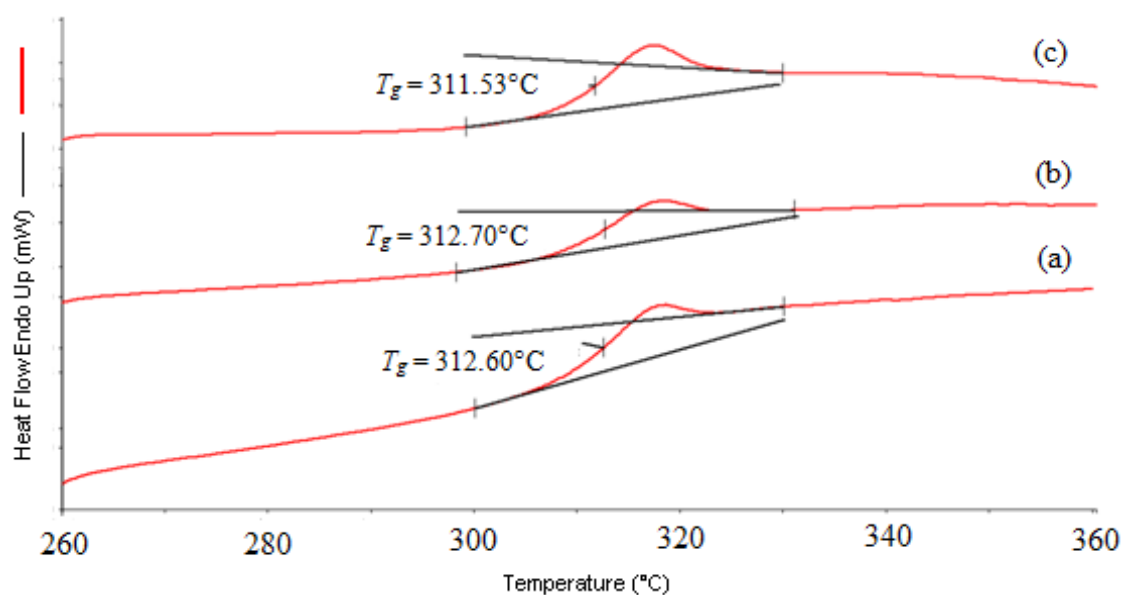
Figure 4.7 : DSC thermograms MMMs containing (a) 5 wt% as-synthesized *sod*-ZMOF, (b) 10 wt% as-synthesized *sod*-ZMOF, (c) 10 wt% Na^+-*sod*-ZMOF particles.

4.2.3 Gas separation properties

Table 4.3 summarizes the average single gas permeabilities and CO_2/CH_4 ideal selectivities for MMMs and also for neat polymer membrane in order to compare the performances.

Table 4.3 : CH_4/CO_2 separation performance of pure Matrimid and MMMs.

Membrane	Permeability (Barrer)		Ideal selectivity
	CH_4	CO_2	
Pure Matrimid®	0.10	3.80	37.8
5% *sod*-ZMOF/Matrimid®	0.13	4.64	36.8
10% *sod*-ZMOF/Matrimid®	0.14	5.12	36.7
10% Na^+-*sod*-ZMOF/Matrimid®	0.12	4.60	38.9

The obtained data indicated that the permeabilities for both gases increased with the incorporation of *sod*-ZMOF particles into the polymer matrix. 5 wt% and 10 wt% *sod*-ZMOF-loaded MMMs confirmed that permeabilities increased as the filler content increased. The increase in the permeability of CO_2 was 35% with 10 wt% *sod*-ZMOF loading while it was 22% for 5 wt% loading. It was also illustrated in Figure 4.8, which presents the permeabilities as a function of *sod*-ZMOF content in Matrimid matrix. The permeability improvement was an expected result as *sod*-ZMOF crystals have extra large cavities (9.6 Å) and generate paths inside the polymer matrix that gas molecules could readily pass through.
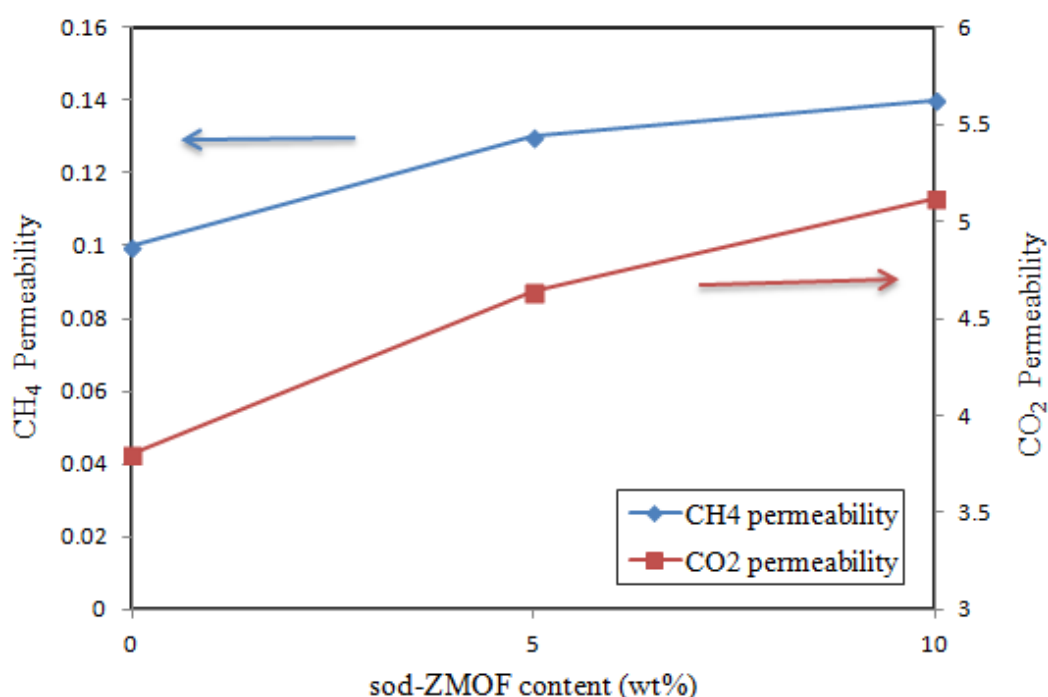
Figure 4.8 : CH_4 and CO_2 permeabilities of Matrimid® membranes as a function of *sod*-ZMOF content.

On the other hand, the ideal selectivities slightly decreased in MMMs (except the one containing ion-exchanged *sod*-ZMOF) compared to the pure polymer membrane. This data could also be explained by the Maxwell model, which assumes that there will be no improvement in selectivity when the gas permeability of the dispersed particle is much larger than that of the polymer matrix. Since these selectivity decreases were relatively negligible, the membrane could be said to be free of interfacial defects, which would have a distinct adverse effect on the selectivity. Hence, the results for MMMs also agrees with the SEM images showing no significant voids at the polymer/filler interface. The membrane which contains ion-

exchanged *sod*-ZMOF exhibited a different behavior from the ones containing as-synthesized *sod*-ZMOF. It showed an increase in the selectivity different from the others. This may be attributed to the differences in electrostatic interaction of different gas molecules with the introduced alkali metal ions (Na^+). Na^+ cations could be said to have higher affinity to CO_2, which has a strong quadrupole moment.

For a better evaluation, the pure-component CO_2 and CH_4 gas transport properties of *sod*-ZMOF-loaded MMMs were illustrated on a Robeson plot in Figure 4.9. It can also be seen on this figure that the incorporation of *sod*-ZMOF particles improved the separation performance of the membranes by increasing the CO_2 permeability without any significant loss in selectivity.
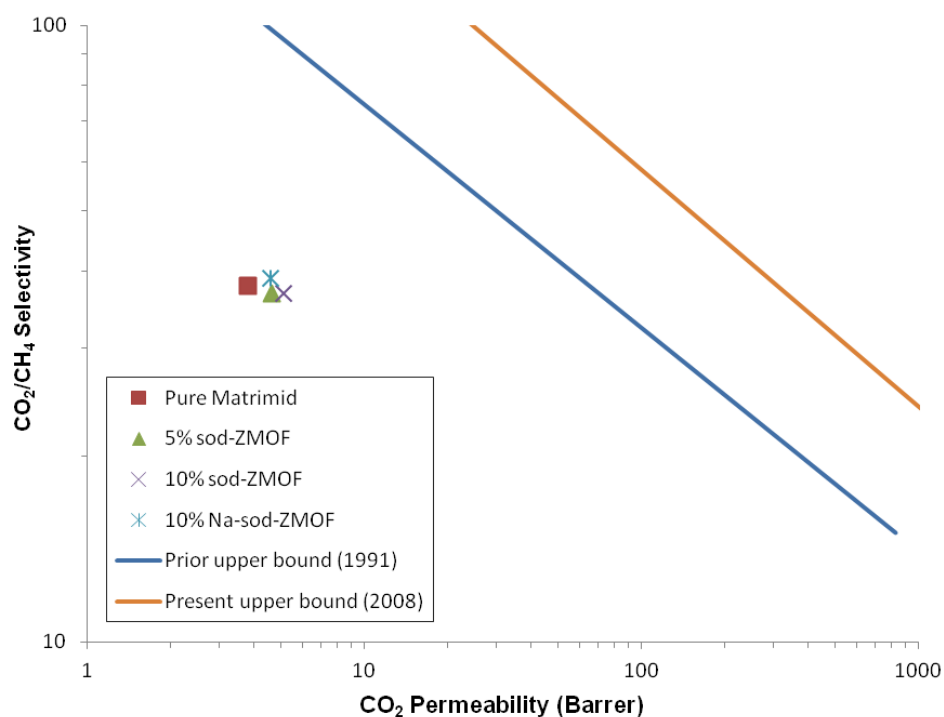
Figure 4.9 : Single gas separation performances of pure Matrimid® membranes and *sod*-ZMOF/Matrimid® MMMs shown on the Robeson diagram [44].

5. CONCLUSIONS

This study focused on the development of MOF/polymer MMMs with the aim of using in natural gas purification applications. *Sod*-ZMOF crystals were synthesized and characterized, then they were incorporated into Matrimid® 5218 matrix. Following the morphological and thermal characterization, gas permeation properties of membranes were also tested at 35°C temperature and 4000 mbar upstream pressure.

The XRD pattern of the MMM showed that *sod*-ZMOF maintained its crystallinity through and after the mechanical and heating processes in the membrane preparation procedure. The SEM images of MMMs showed no apparent voids or defects at the filler/polymer interface and that ZMOF particles were dispersed homogenously in the polymer matrix. This result indicates that there was a good compatibility between the *sod*-ZMOF crystals and the polymer (Matrimid®) matrix, which could be attributed to the partial organic framework of the MOF particles.

The TGA results of membranes showed that almost all of the residual solvent or moisture within the membrane could be evacuated by annealing the membranes at 200°C for 48 h. In addition, DSC results indicated that there was a slight increase in T_g of membranes with incorporation of *sod*-ZMOF particles into the polymer matrix.

The gas permeability measurements indicated that incorporation of *sod*-ZMOF particles into the Matrimid® matrix enhanced the permeabilities with almost no loss of selectivities. They also provide increase both in the CO_2 permeability and selectivity with the opportunity of fine tuning through ion exchange

In conclusion, *sod*-ZMOF type MOFs are seen as promising performance enhancers for polyimide CO_2 separation membranes. Further studies for measuring CO_2/CH_4 binary gas mixture separation properties are assumed to better clarify the performance of these MMMs. Studies will also be performed with MMMs containing higher amounts of *sod*-ZMOF loadings.

REFERENCES

[1] **Koltuniewicz, A., Drioli, E.** (2008). *Membranes in Clean Technologies*. (Vol. 1). Weinheim, Wiley-VCH.

[2] **Koros, W.J., Mahajan, R.** (2000). Pushing the limits on possibilities for large scale gas separation: which strategies?, *Journal of Memnrane Science, 175,* 181-196.

[3] **Mahajan, R.** (2000). Formation, Characterization and modeling of mixed matrix membrane materials, *PhD Thesis,* The University of Texas at Austin.

[4] **Li, Y.** (2006). Development of mixed matrix membranes for gas separation application, *PhD Thesis,* Tsinghua University, P. R. China.

[5] **Nath, K**. (2008). *Membrane Seperation Process : Basic Concepts.* New Delhi, Prentice-Hall.

[6] **Mulder, M.** (1996). *Basic Principles of Membrane Technology* (2nd ed.). Toronto, USA, Kluwer Academic Publishers.

[7] **Goh, P.S., Ismail, A.F., Sanip, S.M., Ng, B.C., Aziz, M.** (2011). Recent advances of inorganic fillers in mixed matrix membrane for gas separation, *Separation and Purification Technology, 81,* 243-264.

[8] **Chung, T.S., Jiang, L.Y., Li, Y., Kulprathipanja, S.** (2007). Mixed matrix membranes (MMMs) comprising organic polymers with dispersed inorganic fillers for gas separation, *Progress in Polymer Science, 32,* 483-507.

[9] **Zhang, Y., Musselman, I.H., Ferraris, J.P., Balkus Jr., K.J.** (2008). Gas permeability properties of Matrimid® membranes containing the metal-organic framework Cu–BPY–HFS, *Journal of Membrane Science, 313,* 170-181.

[10] **Yampolskii, Y., Freeman, B.** (2010). *Membrane Gas Separation.* United Kingdom, John Wiley & Sons Ltd.

[11] **Wallace, D.W.** (2004). Crosslinked hollow fiber membranes for natural gas purification and their manufacture from novel polymers, *PhD thesis,* The University of Texas at Austin.

[12] **Url-1** <http://www.ornl.gov/info/ornlreview/v38_1_05/article06.shtml>, date retrieved 10.11.2012.

[13] **Baker, R.W.** (2004). *Membrane Technology and Applications.* John Wiley & Sons, England.

[14] **Kesting, R.E., Fritzsche, A.K.** (1993). *Polymeric Gas Separation Membranes.* John Wiley & Sons.

[15] **Baker, R.W.** (2002). Future directions of membrane gas separation technology, *Industrial & Engineering Chemistry Research, 41,* 1393-1411.

[16] **Kertik, A.** (2010). Gas purification using polymer/zeolite composite membranes, *MSc Thesis,* Istanbul Technical University, Turkey.

[17] **Oral, E.E.** (2011). Effect of operating parameters on performance of additive/zeolite/polymer mixed matrix membranes, *MSc Thesis,* Middle East Technical University, Turkey.

[18] **Mokhatab, S., Poe, W.A., Speight, J.G.** (2006), *Handbook of Natural Gas Transmission and Processing.* Gulf Proffesional Publishing, USA.

[19] **Wind, J.D.** (2002). Improving polyimide membrane resistance to carbon dioxide plasticization in natural gas separations, *PhD Thesis,* The University of Texas at Austin.

[20] **Jusoh, N.W., Lau, K.K., Shariff, A.M.** (2012). Purification of natural gas with impurities using membrane processes: parameter estimation, *American Journal of Engineering and Applied Sciences, 5(1),* 78-83.

[21] **Beggs, H.D.** (1984). *Gas Production Operations.* Oil & Gas Consultants International Inc.

[22] **Url-2** <http://www.naturalgas.org/environment/naturalgas.asp>, date retrieved 20.11.2012.

[23] **Wind, J.D., Paul, D.R., Koros, W.J.** (2004). Natural gas permeation in polyimide membranes, *Journal of Membrane Science, 228,* 227-236.

[24] **Belmabkhout, Y., Serna-Guerrero, R., Sayari, A.** (2010). Adsorption of CO_2-containing gas mixtures over amine-bearing pore-expanded MCM-41 silica: application for gas purification, *Industrial & Engineering Chemistry Research, 49,* 359-365.

[25] **Keskin, S., Sholl, D.S.** (2010). Selecting metal organic frameworks as enabling materials in mixed matrix membranes for high efficiency natural gas purification, *Energy & Environmental Science, 3,* 343-351.

[26] **Rochelle, G.T.** (2009). Amine scrubbing for CO_2 capture, *Science, 325,* 1652-1654.

[27] **Huang, H.Y., Yang, R.T.** (2003). Amine-grafted MCM-48 and silica xerogel as superior sorbents for acidic gas removal from natural gas, *Industrial & Engineering Chemistry Research, 42,* 2427-2433.

[28] **Baker, R.W., Lokhandwala, K.** (2008). Natural gas processing with membranes: an overview, *Industrial & Engineering Chemistry Research, 47,* 2109-2121.

[29] **Bhide, B.D., Voskericyan, A., Stern, S.A.** (1998). Hybrid processes for the removal of acid gases from natural gas, *Journal of Membrane science, 140,* 27-49.

[30] **Venna, S. R., Carreon, M. A.** (2009). Highly permeable zeolite imidazolate framework-8 membranes for CO_2-CH_4 separation, *Journal of the American Chemical Society, 132,* 76-78.

[31] **Sutherland, K.** (2004). *Profile of the International Membrane Industry: Market Prospects to 2008.* Elsevier Ltd., third edition.

[32] **Scholes, C.A., Kentish, S.E.** (2008). Carbon dioxide separation through polymeric membrane systems for flue gas applications, *Recent Patents on Chemical Engineering, 1,* 52-66.

[33] **Hao, J, Rice, P.A., Stern, S.A.** (2002). Upgrading low-quality natural gas with H_2S- and CO_2-selective polymer membranes_Part I. Process design and economics of membrane stages without recycle streams, *Journal of Membrane Science, 209,* 177-206.

[34] **Sridhar, S., Smitha, B., Aminabhavi, T.M.** (2007). Separation of carbon dioxide from natural gas mixtures through polymeric membranes-a review, *Separation & Purification Reviews, 36,* 113–174.

[35] **Url-3** <http://www.co2crc.com.au/aboutccs/cap_membranes.html>, date retrieved 25.11.2012.

[36] **Yampolskii, Y., Pinnau, I., Freeman, B.** (2006). *Materials Scince of Membranes for Gas and Vapor Separation.* John Wiley & Sons Ltd, England.

[37] **Pandey, P., Chauhan, R.S.** (2001). Membranes for gas separation, *Progress in Polymer Science, 26,* 853-893.

[38] **Dhingra, S.S., Marand, E.** (1998). Mixed gas transport study through polymeric membranes, *Journal of Membrane Science, 141,* 45-63.

[39] **Du, N., Park, H.B., Dal-Cin, M.M., Guiver, M.D.** (2012). Advances in high permeability polymeric membrane materials for CO2 separations, *Energy & Environmental Science, 5,* 7306-7322.

[40] **Yampolskii, Y.** (2012). Polymeric gas separation membranes, *Macromolecules, 45,* 3298-3311.

[41] **Robeson, L.M.** (1999). Polymer membranes for gas separation, *Current Opinion in Solid State & Material Science, 4,* 549-552.

[42] **Freeman, B.D.** (1999). Basis of Permeability/Selectivity Tradeoff Relations in Polymeric Gas Seaparation Membranes, *Macromolecules, 32,* 375-380.

[43] **Cong, H., Radosz, M., Towler, B.F., Shen, Y.** (2007). Polymer–inorganic nanocomposite membranes for gas separation, *Separation and Purification Technology, 55,* 281-291.

[44] **Robeson, L.M.** (2008). The upper bound revisited, *Journal of Membrane Science, 320,* 390-400.

[45] **Scholes, C.A., Stevens, G.W., Kentish, S.E**. (2012). Membrane gas separation applications in natural gas processing, *Fuel, 96,* 15-28.

[46] **Liu, C., Wilson, S.T., Kulprathipanja, S.** (2009). Crosslinked organic-inorganic hybrid membranes and their use in gas separation, *United States Patent,* No: 0299015 dated 3.12.2009.

[47] **Zhao, H-Y., Cao, Y-M., Ding, X-L., Zhou, M-Q., Liu, J-H., Yuan, Q.** (2008). Poly(ethylene oxide) induced cross-linking modification of Matrimid membranes for selective separation of CO2, *Journal of Membrane Science, 320,* 179-184.

[48] **Nemser, S.M., Roman, I.C.** (1991). Perfluorodioxole membranes, *United States Patent,* No:5051114 dated 24.9.1991.

[49] **Ismail, A.F., David, L.I.B.** (2001). A review on the latest development of carbon membranes for gas separation, *Journal of Membrane Science, 193,* 1-18.

[50] **Li, S., Carreon, M.A., Zhang, Y., Funke, H.H., Noble, R.D., Falconer, J.L.** (2010). Scale-up of SAPO-34 membranes for CO_2/CH_4 separation, *Journal of Membrane Science, 352,* 7-13.

[51] **Himeno, S., Tomita, T., Suzuki, K., Nakayama, K., Yajima, K., Yoshida, S.** (2007). Synthesis and permeation properties of a DDR-type zeolite membrane for separation of CO2/CH4 gaseous mixtures, *Industrial & Engineering Chemistry Research, 46,* 6989–6997.

[52] **Vos, R.M., Verweij, H.** (1998). Improved performance of silica membranes for gas separation, *Journal of Membrane Science, 143,* 37-51.

[53] **Perez, E.V., Balkus,cK.J., Ferraris, J.P., Musselman, I.H.** (2009). Mixed-matrix membranes containing MOF-5 for gas separations, *Journal of Membrane Science, 328,* 165-173.

[54] **Zimmerman, C.M., Singh, A., Koros, W.J.** (1997). Tailoring mixed matrix composite membranes for gas separations, *Journal of Membrane Science, 137,* 145-154.

[55] **Cakal, U., Yilmaz, L., Kalipcilar, H.** (2012). Effect of feed gas composition on the separation of CO_2/CH_4 mixtures by PES-SAPO 34-HMA mixed matrix membranes, *Journal of Membrane Science, 417-418,* 45-51.

[56] **Karkhanechi, H., Kazemian, H., Nazockdast, H., Mozdianfard, M.R., Bidoki, S.M.** (2012). Fabrication of homogenous polymer-zeolite nanocomposites as mixed-matrix membranes for gas separation, *Chemical Engineering & Technology, 35,* 885-892.

[57] **Kim, S., Marand, E.** (2008). High permeability nano-composite membranes based on mesoporous MCM-41 nanoparticles in a polysulfone matrix, *Microporous and Mesoporous Materials, 114,* 129-136.

[58] **Sen, D., Kalipcilar, H., Yilmaz, L.** (2007). Development of polycarbonate based zeolite 4A filled mixed matrix gas separation membranes, *Journal of Membrane Science, 303,* 194-203.

[59] **Zhang, Y.F., Balkus, K.J., Musselman, I.H., Ferraris, J.P.** (2008). Mixed-matrix membranes composed of Matrimid® and mesoporous ZSM-5 nanoparticles, *Journal of Membrane Science, 325,* 28-39.

[60] **Duval, J.-M., Kemperman, A.J.B., Folkers, B., Mulder, M.H.V.,** et al. (1994). Preparation of zeolite filled glassy polymer membranes, *Journal of Applied Polymer Science, 54,* 409-418.

[61] **Vu, D.Q., Koros, W.J., Miller, S.J.** (2003). Mixed matrix membranes using carbon molecular sieves_II. Modeling permeation behavior, *Journal of Membrane Science, 211,* 335-348.

[62] **Bae, T.-H., Lee, J.S., Qiu, W., Koros, W.J., Jones, C.W., Nair, S.** (2010). A high-performance gas-separation membrane containing submicrometer-sized metal–organic framework crystals, *Angewandte Chemie International Edition, 49,* 9863-9866.

[63] **Li, H., Eddaoudi, M., O'Keeffe, M., Yaghi, O.M.** (1999). Design and synthesis of an exceptionally stable and highly porous metal-organic framework, *Nature, 402,* 276-279.

[64] **Yehia, H., Pisklak, T. J., Ferraris, J.P., Balkus, K. J., Musselman, I. H.** (2004). Methane facilitated transport using copper (II) biphenyl dicarboxylate-triethylenediamine poly(3-acetoxyethylthiophene) mixed matrix membranes, *Polymer Preprints, 45,* 35-36.

[65] **Li, Y., Liang, F., Bux, H., Yang, W., Caro, J.** (2010). Zeolitic imidazolate framework ZIF-7 based molecular sieve membrane for hydrogen separation, *Journal of Membrane Science, 354,* 48-54.

[66] **Ordonez, M.J.C., Balkus, K.J., Ferraris, J.P., Musselman, I.H.** (2010). Molecular sieving realized with ZIF-8/Matrimid® mixed-matrix membranes, *Journal of Membrane Science, 361,* 28-37.

[67] **Adams, R., Carson, C., Ward, J, Tannenbaum, R., Koros, W.** (2010). Metal organic framework mixed matrix membranes for gas separations, *Microporous and Mesoporous Materials, 131,* 13-20.

[68] **Car, A., Stropnik, C., Peinemann, K.-V.** (2006). Hybrid membrane materials with different metal–organic frameworks (MOFs) for gas separation, *Desalination, 200,* 424-426.

[69] **Mahajan, R., Koros, W.** (2000). Factors controlling successful formation of mixed-matrix gas separation materials, *Industrial & Engineering Chemistry Research, 39,* 2692-2696.

[70] **Jiang, L., Chung, T.-S., Li, D.F., Cao, C., Kulprathipanja, S.** (2004). Fabrication of Matrimid/polyethersulfone dual-layer hollow fiber membranes for gas separation, *Journal of Membrane Science, 240,* 91-103.

[71] **Tin, P.S., Chung, T.S., Liu, Y., Wang, R., Liu, S.L., Pramoda, K.P.** (2003). Effects of cross-linking modification on gas separation performance of Matrimid membranes, *Journal of Membrane Science, 225,* 77-90.

[72] **Vu, D.Q., Koros, W.J., Miller, S.J.** (2003). Effect of condensable impurity in CO_2/CH_4 gas feeds on performance of mixed matrix membranes using carbon molecular sieves, *Journal of Membrane Science, 221,* 233-239.

[73] **Chung, T.-S., Chan, S.S., Wang, R., Lu, Z., He, C.** (2003). Characterization of permeability and sorption in Matrimid/C60 mixed matrix membranes, *Journal of Membrane Science, 211,* 91-99.

[74] **Sridhar, S., Veerapur, R.S., Patil, M.B., Gudasi, K.B., Aminabhavi, T.M.** (2007). Matrimid polyimide membranes for the separation of carbon dioxide from methane, *Journal of Applied Polymer Science, 106,* 1585-1594.

[75] **Bos, A., Pünt, I.G.M., Wessling, M., Strathmann, H.** (1998). Plasticization-resistant glassy polyimide membranes for CO_2/CO_4 separations, *Separation and Purification Technology, 14,* 27-39.

[76] **Zornoza, B., Tellez, C., Coronas, J., Gascon, J., Kapteijn, F.** (2013). Metal organic framework based mixed matrix membranes: An increasingly important field of research with a large application potential, *Microporous and Mesoporous Materials, 166,* 67-78.

[77] **Erucar, I., Keskin, S.** (2011). Screening metalorganic framework-based mixed-matrix membranes for CO_2/CH_4 separations, *Industrial & Engineering Chemistry Research, 50,* 12606-12616.

[78] **Nouar, F., Eckert, J., Eubank, J.F., Forster, P., Eddaoudi, M.** (2009). Zeolite-like metal-organic frameworks (ZMOFs) as hydrogen storage platform: lithium and magnesium ion-exchange and H_2-(rho-ZMOF) interaction studies, *Journal of the American Chemical Society, 131,* 2864-2870.

[79] **Calleja, G., Botas, J.A., Sanchez-Sanchez, M., Orcajo, M.G.** (2010). Hydrogen adsorption over zeolite-like MOF materials modified by ion exchange, *International Journal of Hydrogen Energy, 35,* 9916-9923.

[80] **Chen, C., Kim, J., Yang, D.-A., Ahn, W.-S.** (2011), Carbon dioxide adsorption over zeolite-like metal organic frameworks (ZMOFs) having a sod topology: Structure and ion-exchange effect, *Chemical Engineering Journal, 168,* 1134-1139.

[81] **Park, K.S., Ni, Z., Cote, A.P., Choi, J.Y., Huang, R., Uribe-Romo, F.J.,** et al. (2006). Exceptional chemical and thermal stability of zeolitic imidazolate frameworks, *Proceedings of the National Academy of Sciences, 103,* 10186-10191.

[82] **Shah, M., McCarthy, M.C., Sachdeva, S., Lee, A.K., Jeong, H.-K.** (2012). Current Status of MetalOrganic Framework Membranes for Gas Separations: Promises and Challenges, *Industrial & Engineering Chemistry Research, 51,* 2179-2199.

[83] **Brant, J.A., Liu, Y., Sava, D.F., Beauchamp, D., Eddaoudi, M.** (2006). Single-metal-ion-based molecular building blocks (MBBs) approach to the design and synthesis of metal–organic assemblies, *Journal of Molecular Structure, 796,* 160-164.

[84] **Liu, Y., Kravtsov, V.C., Larsen, R., Eddaoudi, M.** (2006). Molecular building blocks approach to the assembly of zeolite-like metal–organic frameworks (ZMOFs) with extra-large cavities, *Chemical Communications,* 1488-1490.

[85] **Basu, S., Cano-Odena, A., Vankelecom, I.F.J.** (2011). MOF-containing mixed-matrix membranes for CO_2/CH_4 and CO_2/N_2 binary gas mixture separations, *Separation and Purification Technology, 81,* 31-40.

[86] **Clearfield, A., Reibenspies, J.H., Bhuvanesh, N.** (2010). *Principles and applications of powder diffraction.* John Wiley and Sons Ltd, USA.

[87] **Brundle, C.R., Evans, C.A., Wilson, S.** (1992). *Encyclopedia of Materials Characterization.* Butterworth-Heiemann, USA.

[88] **Scanning electron microscope.** (n.d.). In *Wikipedia*, Date retrieved: 30.11.2012, address: http://en.wikipedia.org/wiki/Scanning_electron_microscope

[89] **Hatakeyama, T., Quinn, F.X.** (1994). *Thermal Analysis_Fundamentals and Applications to Polymer Science.* John Wiley & Sons, England.

[90] **Cheremisinoff, N.P.** (1996). *Polymer Characterization-Laboratory Techniques and Analysis.* William Andrew Publishing/Noyes.

CURRICULUM VITAE

Name Surname: Ayşe KILIÇ

Place and Date of Birth: İstanbul / 01.01.1987

Address: İstanbul Technical University, Faculty of Chemical and Metallurgical Engineering, Floor: 5 Room: B-505 34469 Maslak/İSTANBUL

E-Mail: kilicay@itu.edu.tr

                          aysekilic19@yahoo.com.tr

B.Sc.:   İstanbul Technical University
                          Chemical Engineering Department (2005-2010)